ELSEVIER

Neuropsychologia 44 (2006) 2647–2667

NEUROPSYCHOLOGIA

www.elsevier.com/locate/neuropsychologia

Mapping the parietal cortex of human and non-human primates

Guy A. Orban [a,*], Kristl Claeys [a,b,c], Koen Nelissen [a], Ruth Smans [a], Stefan Sunaert [d], James T. Todd [e], Claire Wardak [a], Jean-Baptiste Durand [a], Wim Vanduffel [a]

[a] *Laboratorium voor Neuro- en Psychofysiologie, K.U.Leuven, Medical School, Leuven, Belgium*
[b] *Laboratorium voor Theoretische Neurobiologie, University Antwerp, Antwerp, Belgium*
[c] *Division of Neurology, University Hospital Antwerp, Antwerp, Belgium*
[d] *Division of Radiology, UZ Gasthuisberg, Leuven, Belgium*
[e] *Department of Psychology, Ohio State University, Columbus, OH, United States*

Received 2 June 2005; received in revised form 13 October 2005; accepted 1 November 2005
Available online 12 December 2005

Abstract

The present essay reviews a series of functional magnetic resonance imaging (fMRI) studies conducted in parallel in humans and awake monkeys, concentrating on the intraparietal sulcus (IPS). MR responses to a range of visual stimuli indicate that the human IPS contains more functional regions along its anterior–posterior extent than are known in the monkey. Human IPS includes four motion sensitive regions, ventral IPS (VIPS), parieto-occipital IPS (POIPS), dorsal IPS medial (DIPSM) and dorsal IPS anterior (DIPSA), which are also sensitive to three-dimensional structure from motion (3D SFM). On the other hand, the monkey IPS contains only one motion sensitive area (VIP), which is not particularly sensitive to 3D SFM. The human IPS includes four regions sensitive to two-dimensional shape and three representations of central vision, while monkey IPS appears to contain only two shape sensitive regions and one central representation. These data support the hypothesis that monkey LIP corresponds to the region of human IPS between DIPSM and POIPS and that a portion of the anterior part of human IPS is evolutionarily new. This additional cortical tissue may provide the capacity for an enhanced visual analysis of moving images necessary for sophisticated control of manipulation and tool handling.

Keywords: Visual; Cerebral cortex; Homology; Functional imaging

1. Introduction

The parietal cortex is a typical higher order multimodal cortex, receiving visual, somatosensory and auditory signals. It is generally believed that its main function is the transformation of sensory signals into motor signals. Parietal cortex is much expanded in humans compared to macaques: while the overall cerebral cortex surface of humans amounts to 10 times that of the macaque, this ratio is at least twice as large for the lower part of the parietal cortex, the inferior parietal lobule (IPL) (Orban, Van Essen, & Vanduffel, 2004; Van Essen, 2004). The present review is restricted to the part of parietal cortex devoted to vision, which is generally referred to as posterior parietal cortex (PPC). With the advent of functional imaging the human parietal cortex has received considerable attention. Motor tasks have been tested, in the earlier PET studies (Faillenot, Toni, Decety, Gregoire, & Jeannerod, 1997; Grafton, Fagg, Woods, & Arbib, 1996; Lacquaniti et al., 1997; Petit et al., 1993; Pierrot-Deseilligny, Rivaud, Gaymard, & Agid, 1991; Rizzolatti et al., 1996) but also in the more recent fMRI studies (e.g. Astafiev et al., 2003; Binkofski et al., 1999; Connolly, Andersen, & Goodale, 2003; Muri, Iba-Zizen, Derosier, Cabanis, & Pierrot-Deseilligny, 1996; Petit & Haxby, 1999). Most fMRI studies of PPC, however, have focused on cognitive tasks, or on passive sensory stimulation and simple discriminations (Claeys et al., 2004; Shikata et al., 2001; Shulman et al., 1999). This profusion of studies has revealed that parietal cortex is involved in a surprisingly large series of cognitive functions including motor planning, spatial and other types of attention, visual and non-visual working memory, spatial representation and coordinate transformation, mental rotation, task relevant processing, calculation and even aspects of long term memory and language (Shannon & Buckner, 2004; Simon, Mangin, Cohen, Le Bihan, & Dehaene, 2002; for review

* Corresponding author. Tel.: +32 16 34 57 44; fax: +32 16 34 59 93.
E-mail address: guy.orban@med.kuleuven.be (G.A. Orban).

0028-3932/$ – see front matter © 2005 Elsevier Ltd. All rights reserved.
doi:10.1016/j.neuropsychologia.2005.11.001

Behrmann, Geng, & Shomstein, 2004; Culham & Kanwisher, 2001).

Even if one considers the function that has been most explored in the IPS, attention, progress has nonetheless been rather slow. Moreover, most results are simply reported in extremely coarse anatomical terms, e.g. anterior versus posterior intraparietal sulcus (IPS), SPL versus IPL. Recently, it has become clear that different parietal regions may be involved in the automatic attraction of attention and its voluntary control (Behrmann et al., 2004; Corbetta, Kincade, Ollinger, McAvoy, & Shulman, 2000; Corbetta, Kincade, & Shulman, 2002), or in shifting and maintaining spatial attention (Vandenberghe, Gitelman, Parrish, & Mesulam, 2001; Yantis et al., 2002). Finally a series of studies (Corbetta et al., 1998; Beauchamp, Petit, Ellmore, Ingeholm, & Haxby, 2001; Perry & Zeki, 2000; Vandenberghe et al., 2001) have underscored the similarity of the regions involved in covert and overt shift in attention, in agreement with the influential premotor theory of attention (Rizzolatti, Riggio, Dascola, & Umilta, 1987).

In contrast to human parietal cortex, which is still poorly understood, that of the macaque is known to contain a restricted number of cortical areas. In particular, the lateral intraparietal (LIP) region (Andersen, Bracewell, Barash, Gnadt, & Fogassi, 1990) and the posterior reach region (PRR), including V6A and the medial intraparietal (MIP) region, have been a focus of single cell investigations (Andersen & Buneo, 2002; Batista & Andersen, 2001; Fattori, Gamberini, Kutz, & Galletti, 2001; Ferraina, Pare, & Wurtz, 2002). Although the exact parcellation of monkey PPC and the precise limits of most areas are still in debate (Van Essen, 2004), a coherent picture of the sensorimotor and related cognitive functions implemented by the PPC, is beginning to emerge (for reviews Andersen & Buneo, 2002; Gold and Shadlen, 2003; Rizzolatti & Luppino, 2001). A brief, speculative, but thought-provoking description goes as follows. In general, the parietal cortex uses sensory inputs to plan one or a series of actions, when the goal and the task have already been decided (by other regions). To that end the PPC needs to deploy a series of capabilities. We speculate that during the course of evolution these capabilities have adapted to operate across a range of behavioral conditions other than strict sensory-motor control, thereby becoming more autonomous and giving rise to the many cognitive functions in which the human PPC appears to be involved.

First, neuronal populations within the PPC must receive the appropriate external signals to operate upon and keep track of the behavioral goal and task (decided by other regions), hence the PPC's role in the control of selection or attention and the task related processing (Assad, 2003; Gottlieb, 2002). Second, the PPC has to process the appropriate features of the sensory signals. For simple motor acts, like reaching or making saccades, position may be sufficient. However, it will be important to represent space in the appropriate coordinate system (eye-centered, head-centered, etc.), hence the functions of spatial representation and coordinate transformations (Andersen & Buneo, 2002). For other actions, e.g. pursuit and catching, the derivative of position over time, i.e. motion, will be critical (Churchland & Lisberger, 2005; Claeys, Lindsey, De Schutter, & Orban, 2003; Indovina et al., 2005). For still other actions, such as grasping, manipulation, tool use, more complex sensory features such as orientation in space, size, 2D and 3D shape will be important (Goodale & Milner, 1992; Iriki, Tanaka, & Iwamura, 1996; Murata, Gallese, Luppino, Kaseda, & Sakata, 2000; Sakata, Taira, Murata, & Mine, 1995; Sereno & Maunsell, 1998; Vanduffel et al., 2002). Third, to decide among choices, prior probabilities and their value or utility will have to be integrated (Platt & Glimcher, 1999; Shadlen & Newsome, 2001; Sugrue, Corrado, & Newsome, 2005), hence the decision processing in the PPC. This integration usually develops over time, hence the delay activity, that may underlie working memory and temporal processing in the PPC (Cornette, Dupont, Salmon, & Orban, 2001; Janssen & Shadlen, 2005; Smith & Jonides, 1999). Fourth, a number of actions will require coordinating the movements of different body parts, e.g. eyes and head, eyes and hand or both hands, hence the eye-hand and other coordination functions (Andersen & Buneo, 2002; Committeri et al., 2004; Puttemans, Wenderoth, & Swinnen, 2005; Vidal, Amorim, & Berthoz, 2004). Finally, in many instances a series of actions will be required, calling for integration of the successive actions (Fogassi et al., 2005) and the evaluation of the result from the previous action by integration of visual and haptic signals, hence the action planning and multimodal integration (Grefkes, Weiss, Zilles, & Fink, 2002; Johansson, Westling, Bäckström, & Flanagan, 2001). Thus the sensory control of action has required the development of a number of computational competences that may have been applied in other behavioral contexts, evolving to yield the complexity of cognitive functions in which the human PPC participates.

The success of single cell studies have prompted many researchers to call for integration of human functional imaging (Culham & Kanwisher, 2001; Glimcher, 2003; Treue, 2003) with the single cell studies in the monkey. This however requires that two issues be resolved: the relationship between fMRI and neuronal signals (Logothetis, Pauls, Augath, Trinath, & Oeltermann, 2001) and the homologies between cortical areas in the two species (Kaas, 2002; Krubitzer & Kahn, 2003; Sereno & Tootell 2005) need to be established. Both problems can be significantly advanced (Orban, 2002) by the use of fMRI in the awake monkey (Vanduffel et al., 2001). To address neuronal operations in higher order cortex such as PPC, it is essential that the monkey subjects are awake. Indeed anesthesia severely depresses neuronal activity in higher order cortex. Therefore, one aim is to review a series of awake monkey fMRI studies which relate to parietal cortex (Denys et al., 2004a,b; Koyama et al., 2004; Sawamura, Georgieva, Vogels, Vanduffel, & Orban, 2005; Tsao et al., 2003; Vanduffel et al., 2001, 2002). It is, however, highly unlikely that all human areas will turn out to have a monkey counterpart. Indeed it would imply that individual cortical areas, like the overall cortical surface, are 10 times larger in humans than in monkeys. This is not an attractive proposal, given the limitations of connection lengths and hence optimal area size. One thus faces the limitations of the monkey model (Behrmann et al., 2004). But even within these restrictions, the parallel study of human and monkey cortex should be extremely beneficial. Charting the homologous areas will provide the beginnings of a map (a

protomap) of human PPC allowing imaging results to be reported in a much more detailed and meaningful way. Furthermore, these homologous areas can act as seeds for understanding neighboring, newly emerged cortex in humans. Indeed for homologous areas, the knowledge derived from single cell studies provides a mechanistic description of the neuronal function localized with the fMRI. This knowledge of neuronal operations can then be extrapolated to evolutionary new cortex, which, presumably enhances and transforms the processing performed in the more basic, homologous regions, with the fMRI indicating the nature of this transformation. Thus a second aim of the review is to further investigate those human functional regions that appeared quite different from their monkey counterparts in our first direct inter-species comparisons in the realm of motion and 3D structure from motion processing (Orban et al., 2003; Vanduffel et al., 2002). In the discussion we will attempt a first outline of a human PPC map, distinguishing evolutionarily old from new areas.

2. Methods

The detailed description of the methods is given in the original papers (Denys et al., 2004a; Fize et al., 2003; Orban, Sunaert, Todd, Van Hecke, & Marchal, 1999; Peuskens et al., 2004; Sawamura et al., 2005; Sunaert, Van Hecke, Marchal, & Orban, 1999; Vanduffel et al., 2001, 2002). Here we only provide a brief summary.

2.1. Subjects

All human subjects had normal or corrected to normal vision and no history of neurological or psychiatric disease, and were drug free. The studies were approved by the Ethical Committee of the K.U.Leuven Medical School, and subjects gave their written informed consent, in accordance with the Helsinki Declaration. Human subjects viewed the stimuli through a mirror tilted at 45° that was attached to the head coil. Subjects were immobilized using an individually molded bite-bar. They were instructed to maintain fixation on a small red target in the center of the screen. Fixation was monitored during all the experiments using a MR-compatible infrared eye movement tracking device (Ober 2, Permobil Meditech AB, Timra, Sweden).

Six male rhesus monkeys (M1, M3-5, M7, M11, *Macaca mulatta*) also served as subjects. All animal care and experimental procedures met the national and European guidelines and were approved by the ethical committee of the K.U.Leuven medical school. The details of the surgical procedures, training of monkeys, image acquisition, eye monitoring and statistical analysis of monkeys scans have been described previously (Denys et al., 2004a; Fize et al., 2003; Vanduffel et al., 2001). The monkey subjects sat in a sphinx position in a plastic monkey chair directly facing the screen. During training they were required to maintain fixation within a 2° × 2° window centered on a red mark in the middle of the screen. Eye position was monitored through the pupil position and corneal reflection (RK-726PCI, Iscan, Cambridge, MA).

Before each monkey scanning session, a contrast agent, monocrystalline iron oxide nanoparticle (MION), was injected into the femoral or external saphenous vein (4–11 mg/kg). While blood oxygenation level-dependent (BOLD) measurements used in humans depend on three hemodynamic variables (blood flow, blood volume and oxygenation level), MION measurements depend only on blood volume. For the sake of clarity, the polarity of the MION MR signal changes, which are opposite to those of BOLD measurements, were inverted.

2.2. Stimuli and tasks

Stimuli were projected by means of a liquid crystal display (LCD) projector (Barco Reality 6300, spatial resolutions ranging from 640 × 480 pixels to 1280 × 1024 in the human experiments, and 1024 × 768 pixels in monkey experiments, at 60 Hz) onto a translucent screen, positioned in the bore of the magnet at 28 cm from the human subjects' eyes (54 cm for monkeys). The experiments used block designs with the presentation order of the conditions randomized between different time series.

The stimuli were intended to probe basic visual processing such as that of motion and shape (both two- and three-dimensional), which are important parameters for visual control of body movements. Motion sensitivity was revealed by contrasting a moving with a static random texture pattern (RTP, 3 × 3 minarc pixels 50% density, 6°/s, 8 random directions, 7° diameter, Sunaert et al., 1999). In experiments described here the diameter and position of the RTP were manipulated. Similar tests using an RTP (0.075° dots, 14° diameter) were also performed on the monkeys, as described in Denys et al. (2004a) and Vanduffel et al. (2001). Recently the motion localizer has been replaced by a speed test in which 5 speeds of motion (1, 2, 4, 8 and 16°/s) were presented. The sensitivity to 3D structure from motion (3D SFM) was studied (see website: http://www.kuleuven.be/neuro) with random line displays in humans (Orban et al., 1999; Vanduffel et al., 2002) and in monkeys (Vanduffel et al., 2002, present experiments). In subsequent human studies random line and random dot displays were used (present experiments) as well as randomly deformed spherical objects (Peuskens et al., 2004).

To map shape sensitive regions in both species, we (Denys et al., 2004a) used grayscale images and drawings (12 × 12 visual degrees) of familiar and non-familiar objects as well as scrambled versions of each set, which were exact copies of those used by Kourtzi and Kanwisher (2000). In addition, we used smaller shape stimuli in the Sawamura et al. (2005) study. These stimuli were gamma-corrected, grayscale images of isolated, mostly man-made objects (average about 4.6° × 4.6°) and phase scrambled versions of these images. In the monkeys and a number of human subjects, retinotopic organization was charted as described in Fize et al. (2003) and Denys et al. (2004a).

Unless stated otherwise, experiments were performed under conditions of passive fixation. Human and monkey subjects made few saccades during scanning and the number of saccades did not differ significantly among conditions.

In a number of studies human and monkey subjects performed a high acuity task (Vanduffel et al., 2001) while being scanned in the experiments. They were required to interrupt an infrared beam with one hand (monkeys) or the index finger (humans) when a small green bar, presented in the center of the screen, changed orientation from horizontal to vertical. In most control experiments the bar size was adjusted in such a way that performance levels were high, averaging 90% correct or better in both species. Recently (Sawamura et al., 2005), in order to demonstrate that attention could be controlled by this paradigm, we systematized our informal observations that bar size allowed us to control the difficulty of the acuity task and hence the attention subjects were allocating to the central bar. We were able to show that performance level, in terms of percent correct detection, decreased significantly with decreasing bar size in both species, while reaction times increased significantly with decreasing bar size. These data allowed us to select a bar size for scanning for which performance would be a sensitive indicator of the subjects' attentional state.

2.3. Data collection and analysis

The data were collected with 1.5 T (Siemens, Sonata) MR scanner. Each functional volume consisted of gradient-echoplanar whole brain images TR = 3.01 s in humans (2.4 s in monkey); TE 50 ms in humans (27 ms in monkeys), flip angle 90°, 64 × 64 matrix, 32 sagittal slices (3 mm × 3 mm × 4.5 mm in humans, 2 mm × 2 mm × 2 mm in monkeys). In the most recent human experiments, we used a 3 T (Philips Intera) MR scanner. Gradient-echoplanar whole brain images were acquired every 3 s (TR = 3000 ms), 64 × 64 matrix, slice thickness 2.5 mm, 50 transverse slices, flip angle 90°. For each subject a high-resolution (1 mm^3) anatomical image (3D-MPRAGE) was acquired.

Human data were analyzed with SPM99 software (Wellcome Department of Cognitive Neurology, London, UK). Preprocessing steps included realignment, co-registration of the anatomical images to the functional scans, and spatial normalization into a standard space. The functional volumes were subsampled to 3 mm × 3 mm × 3 mm for the group and 2 mm × 2 mm × 2 mm for single subject analysis and spatially smoothed with a Gaussian kernel (full width at half height (FWHH) for group analysis: 8 mm; for single subject analysis: 6 mm) prior to statistical analysis. Group data were analyzed with fixed or random effects. Single subject analyses were performed for the comparisons across tasks.

Monkey data, restricted to runs in which monkeys fixated for more than 85% of the time, were analyzed using the SPM 99 and Match software (Chef d'Hotel, Hermosillo, & Faugeras, 2002). In these analyses eye movement parameters and realignment parameters were included as covariates of no interest to reduce eye movement and brain motion artifacts. The monkey functional volumes were realigned and non-rigidly co-registered with the anatomy of M3 as a template in both the group and single subject analyses using a customized volume-based registration algorithm, implemented in the Match software (Chef d'Hotel et al., 2002). In all studies published so far M3′s brain was used as template, but in the more recent analyses we have used the brain of M12 as template, because it has been scanned at higher spatial resolution (0.04 mm^3). The monkey functional volumes were then subsampled to 1 mm^3 and smoothed with an isotropic Gaussian kernel (FWHH 1.5 mm). Each stimulus epoch was represented as a box-car model convoluted by the MION response function as defined by Vanduffel et al. (2001) and Leite et al. (2002). As in humans fixed effects group analyses and single subject analyses were performed.

The threshold of T-score maps was set at $P<0.05$ corrected for multiple comparisons in fixed effects analysis and at $P<0.0001$ uncorrected for multiple comparisons for the random effects analysis. In the single subjects, threshold was set at $P<0.001$ uncorrected for multiple comparisons in humans and $P<0.05$ corrected in monkeys. T-score maps were projected onto the flattened cortical reconstruction (at the level of layer 4) of human brains or the brain of monkey M3 (M12) using the Freesurfer software.

3. Results

3.1. Four motion sensitive regions in human PPC: functional properties

We established that human IPS contains four motion sensitive regions (Orban et al., 2003; Sunaert et al., 1999). Their locations are shown on the flatmap of a single human subject in Fig. 1A. The most posterior of these, the ventral IPS (V*IPS*) region, is located in the occipital part of the intraparietal sulcus (IPS), just dorsal to hV3A. The second is located at the confluence of the occipital and parietal parts of the IPS with the parieto-occipital sulcus (POS) and hence is referred to as parieto-occipital IPS (PO*IPS*) region. The third and fourth motion sensitive regions are located in the parietal or horizontal segment of IPS and thus more dorsally in the brain, hence they are referred to as dorsal IPS medial and anterior (D*IPS*M and D*IPS*A), with DIPSA located anterior in the IPS near the junction with the post-central sulcus. These studies also have shown that responses to flicker (pure temporal change rather than spatio-temporal change typical of motion) gradually decreased along the IPS, being absent in the most dorsal regions (Braddick, O'Brien, Wattam-Bell, Atkinson, & Turner, 2000; Claeys et al., 2003). VIPS is likely similar to what Shulman et al. (1999) refer to as vIPS and Silver, Ress, and Heeger (2005) as IPS1. It may also correspond to IPTO of Wojciulik and Kanwisher (1999). DIPSM is close to what Shulman et al. (1999) and Corbetta et al. (2000) refer to as aIPS and Wojciulik and Kanwisher (1999) as AIPS. Unfortunately what is designated as anterior in the IPS can vary widely amongst studies. It is noteworthy that in our original study (Sunaert et al., 1999) we described two motion sensitive regions, dorsal IPS medial and lateral (DIPSM and DIPSL), the former slightly more medial and posterior than the latter. Subsequently we found this distinction difficult to maintain given the resolution of the fMRI. However, several other studies, e.g. Shulman et al. (1999), Corbetta et al. (2000, 2002) make a similar distinction between what they refer as posterior and anterior IPS.

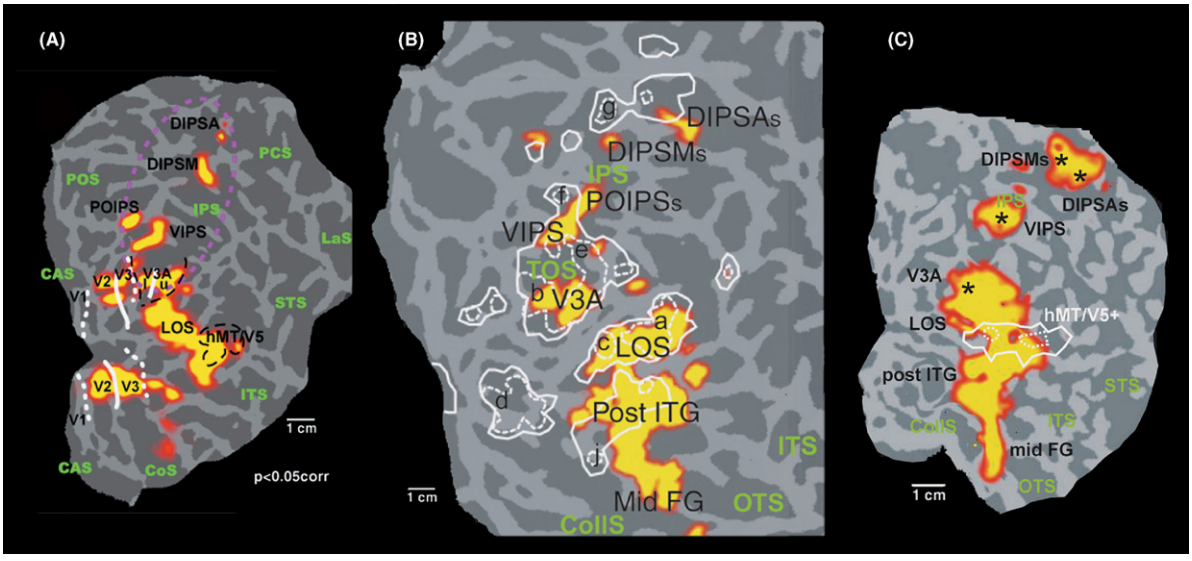

Fig. 1. Flatmaps of the occipital part of human right cerebral hemisphere with statistical parametric maps (SPMs) indicating the four human motion sensitive IPS regions: VIPS, POIPS, DIPSM and DIPSA and their shape sensitive counterparts (POIPSs, DIPSMs and DIPSAs). (A) SPMs plotting voxels significantly ($P<0.05$ corrected, single subject) more active when a human views 3D shape from motion displays compared to 2D controls (from Vanduffel et al. (2002)); (B) SPMs plotting voxels significantly more active when subjects ($n=16$) view intact compared to scrambled shapes (from Denys et al. (2004a,b)); (C) SPMs plotting voxels significantly more active when subjects ($n=6$) view intact compared to phase scrambled shapes, smaller stimuli and taken from a different database (see Section 2) than those in B (from Sawamura et al. (2005)). In (A) solid and stippled white lines indicate horizontal and vertical meridians respectively and black stippled lines motion sensitive regions; in (B) and (C) white solid and stippled lines indicate motion sensitivity at two threshold levels. In (B), letters label local maxima of motion sensitive regions and asterisks in (C) those of shape sensitive regions V3A to DIPSAs. In (A)–(C), sulci are indicated by green abbreviations: CAS: calcarine sulcus, CoS or CollS: collateral sulcus, OTS: occipito-temporal sulcus, ITS: inferior temporal sulcus, STS: superior temporal sulcus, LaS: lateral sulcus, PCS: postcentral sulcus, IPS: intraparietal sulcus, POS: parieto-occipital sulcus, TOS: transverse occipital sulcus.

The coordinates in Talairach space of these four motion sensitive regions are indicated in the 2003 review (Orban et al., 2003, see also Claeys et al., 2003). The distance between these regions is on the order of 15–20 mm. A recent cytoarchitectonic study of human IPS (Choi et al., in press) indicates that the distance between two neighboring regions IPS regions (hIP1 and hIP2) is of the same order of magnitude. Hence we interpret these four motion sensitive regions as indicating the presence of four different cortical areas processing motion information. Much of the remainder of this review then attempts to address three questions raised by this interpretation: (1) is there additional evidence supporting the definition of four cortical areas in human IPS, (2) why does the human brain include four such regions and (3) what is the possible relationship of these regions to monkey IPS areas such as LIP or VIP.

Additional evidence indicating that the two dorsal motion sensitive regions, DIPSM and DIPSA, are situated further along the motion processing chain compared to VIPS and POIPS, was obtained in a recent study contrasting first- and second-order motion to higher order, saliency driven motion (Claeys et al., 2003). The former but not the latter two regions were unresponsive to flickering dots and to invisible motion signals (isoluminant–isosalient moving grating stimuli). This confirms the importance of testing not just *non-motion* stimuli evoking *motion* perception (Enigma, Zeki, Watson, & Frackowiak, 1993) but also *dynamic* stimuli that do *not* evoke motion perception in order to identify cortical regions involved in motion perception. The study by Claeys et al. (2003) also indicated that all four motion sensitive IPS regions were in fact lower order motion regions in the sense of being driven by motion energy. One region located in the IPL was found to be specifically devoted to the processing of saliency-based higher order motion (Claeys et al., 2003). In contrast, attentive tracking, such as tracking multiple balls, simply increases activity in the lower order IPS regions (Culham et al., 1998). More recently these authors have differentiated between an anterior IPS region sensitive to the load in the tracking task and a more posterior region activated by the task independently of the load (Culham, Cavanagh, & Kanwisher, 2001). Unfortunately anatomical localization was only coarsely reported so that the relationship with the four motion sensitive IPS regions is hard to establish.

3.2. Human IPS: further observations on 3D SFM

A first pair of studies (Orban et al., 1999; Vanduffel et al., 2002) addressing the extraction of three-dimensional structure from motion (3D SFM) revealed that the four motion sensitive regions of human IPS are also sensitive to 3D SFM. This is part of an ongoing program to chart in both species the regions involved in extracting 3D structure from the four visual cues: stereo, motion, texture and shading. The 3D structure of objects and the 3D layout of the environment are important visual information for controlling body movements such as grasping or locomotion. Since the first studies suggested that 3D SFM might help answering the questions raised above, we have performed several follow-up studies. For example, Orban et al. (1999) crossed rigidity of motion and dimensionality of shape (3D versus 2D shape) as factors of a factorial design using random line stimuli. In a second study, reported here, we crossed dimensionality of shape with transparency using both random line and random dot stimuli, which are commonly used in single cell studies (Bradley, Chang, & Andersen, 1998; Dodd, Krug, Cumming, & Parker, 2001). The experimental design included eight main conditions, in which opaque or transparent patterns of dots or lines underwent 2D translation or 3D rotation in all possible combinations. Control conditions involved static and (in the plane) rotating lines, static and scrambled moving dots (opaque and transparent) and fixation only. The displays were designed so that the average image plane velocities, and line lengths would be approximately equal in all of the conditions.

The main effect of dimensionality (3D–2D shape) was significant ($P < 0.05$ corrected for multiple comparisons) in hMT/V5+ and in posterior ITG of the right hemisphere. Restricting the effect of dimensionality (3D–2D shape) to opaque surfaces yielded a significant activation in right DIPSA, restricting it to random dot surfaces revealed a significant activation in mid-OTS (Fig. 2).

In addition to this unrestricted spatial analysis we probed the 15 regions defined in the initial experiment (Orban et al., 1999) for the main effect of dimensionality (3D–2D shape), the single effects of dimensionality for opaque and transparent surfaces separately (but pooled over lines and dots) and the effect of dimensionality for opaque dot surfaces (Table 1). The main effect of dimensionality was significant in MT/V5+, mid-OTS, DIPSA and DIPSM. In all regions, except mid-OTS, the effect of dimensionality was much stronger for opaque than transparent surfaces, the interaction reaching significance in MT/V5 and DIPSA. Thus this study indicates that the parietal regions strongly favor opaque surfaces, while the ventral mid-OTS operates equally on the opaque and transparent surfaces. It also further differentiates the four IPS motion regions: (1) the two dorsal ones (DIPSM and DIPSA) are much more involved with 3D SFM than the two ventral ones; (2) the most ventral one, VIPS, favors dots over lines, with the most anterior one, DIPSA, favors lines over dots, the two intermediate regions falling somewhere between. These results not only generalize our initial report (Orban et al., 1999), but also suggest that the differences with other studies can be largely attributed to differences in the stimuli (which are often neglected). Indeed the VIPS and POIPS regions, significantly activated by opaque dot surfaces, are located near the occipito-occipital junction, where Paradis et al. (2000), using opaque dots surfaces and a scrambled control, obtained significant effects of 3D SFM.

The present experiment and the earlier experiments (Orban et al., 1999; Vanduffel et al., 2002), in which the subject remained passive with respect to the stimuli, amply demonstrate the involvement of the four IPS motion regions in extracting 3D SFM. However, in these passive experiments the 3D displays necessarily included a 3D motion aspect in addition to the 3D shape from motion aspect. To disentangle these two aspects we performed an active experiment (Peuskens et al., 2004), in which subjects made judgments about 3D shape, 3D motion and texture of the surface, in addition to dimming detection control

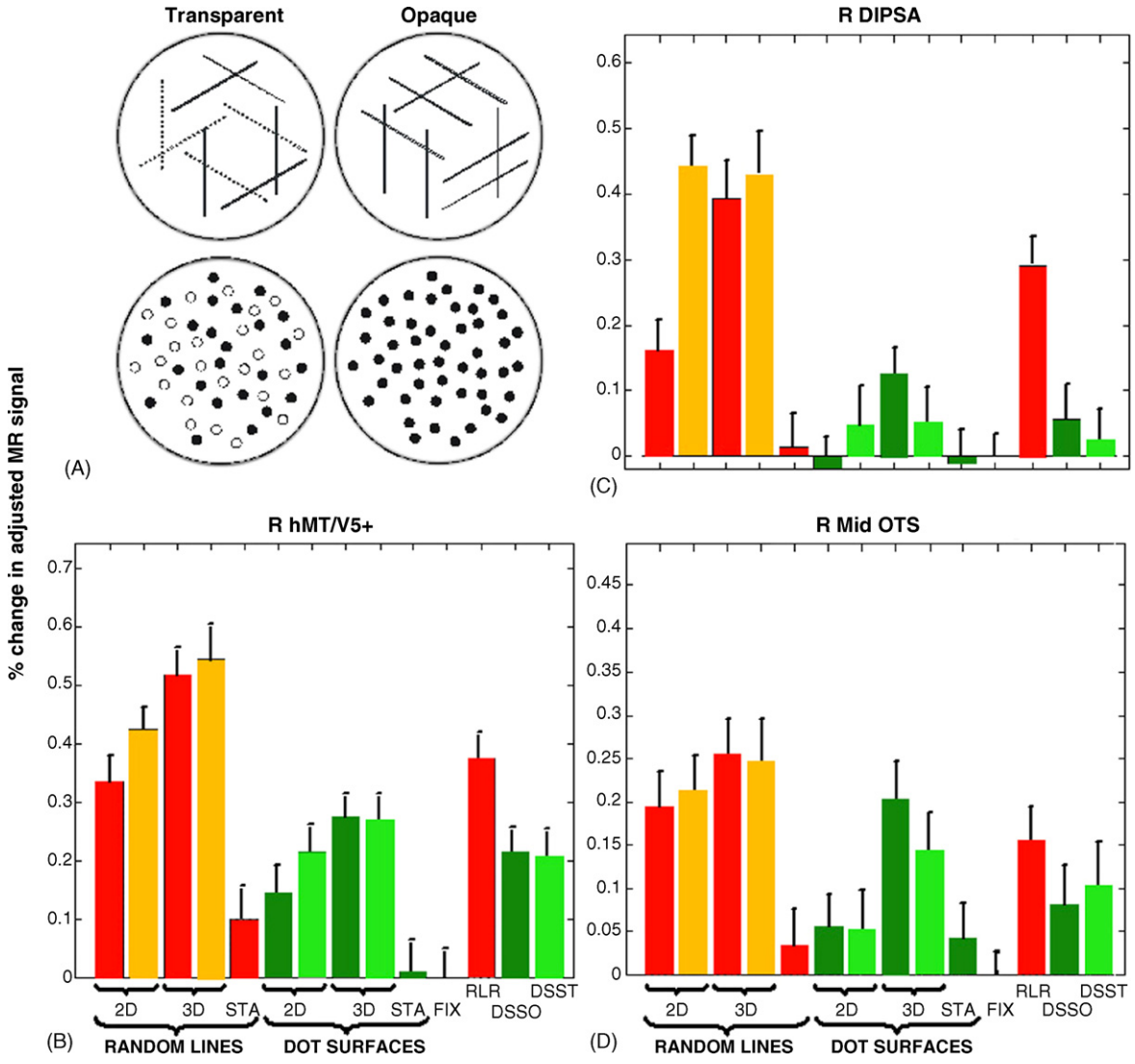

Fig. 2. 3D SFM transparency study. (A) line and dot displays that undergo 3D rotation or 2D translation. The nine random (position and orientation) lines and 720 random (position) dots (life time 30 frames) moved at 3°/s in a circular aperture (9.9 diameter) in the center of the display. Lines (average projected length 4.5°) were constrained to lie on the faces of a randomly oriented cube centered in the aperture. Dots were constrained to lie on the surface of a sphere of the same diameter as the aperture. Lines and dots either rotated in depth around a vertical axis or translated in the plane. Open circles and stippled lines indicated lines and dots located on the back of the 3D object and moved in the opposite direction with respect to those on the front of the object. (B)–(D) activity profiles of h MT/V5+ (B), DIPSA (C) and mid-OTS (D) in right hemisphere: the % MR signal change (group of six subjects) compared to fixation is plotted for the 14 conditions analyzed. Red/orange bars indicate line surfaces, green bars dot surfaces; opaque conditions are in red and dark green, transparent ones in orange and light green. Sta: stationary, fix: fixation, RLR random lines rotating in the image plane, DSSO and DSST: dot surfaces scrambled (vertical positions of dot trajectories) opaque and transparent (appear as a cloud of dots randomly distributed in a volume). Vertical bars indicate S.E.M.

Table 1
Group analysis main effects for 7 of the 15 activation sites of Orban et al. (1999)

Region	Coordinates[a]			Main effect	Single effects		Other subtractions	
	x	*y*	*z*	3D–2D[b]	3D–2D opaque	3D–2D trans	3D–2D dots (opaque)	3D–Scr D (opaque)
R hMT/V5+	52	−62	−2	**5.63**	**5.12**	**2.86**[c]	**3.04**	1.42
R V3A	30	−86	18	2.27	**2.93**	0.28	2.09	1.64
R VIPS	28	−80	36	2.30	2.66	0.59	**2.84**	**2.96**
R POIPS	22	−82	38	1.21	1.80	−0.08	1.75	**2.86**
R DIPSM	30	−50	70	**3.66**	**4.05**	1.13	**2.88**	1.36
R DIPSA	32	−46	70	**3.12**	**4.48**	−0.09[c]	2.53	1.21
R mid-OTS	50	−62	−16	**3.81**	**2.97**	**2.42**	**3.17**	**2.92**

[a] Obtained by searching the (3 × 3) main effect 3D–2D.
[b] Bold $z > 2.72$ ($P < 0.05$ corrected for 15 comparisons).
[c] Significant interaction.

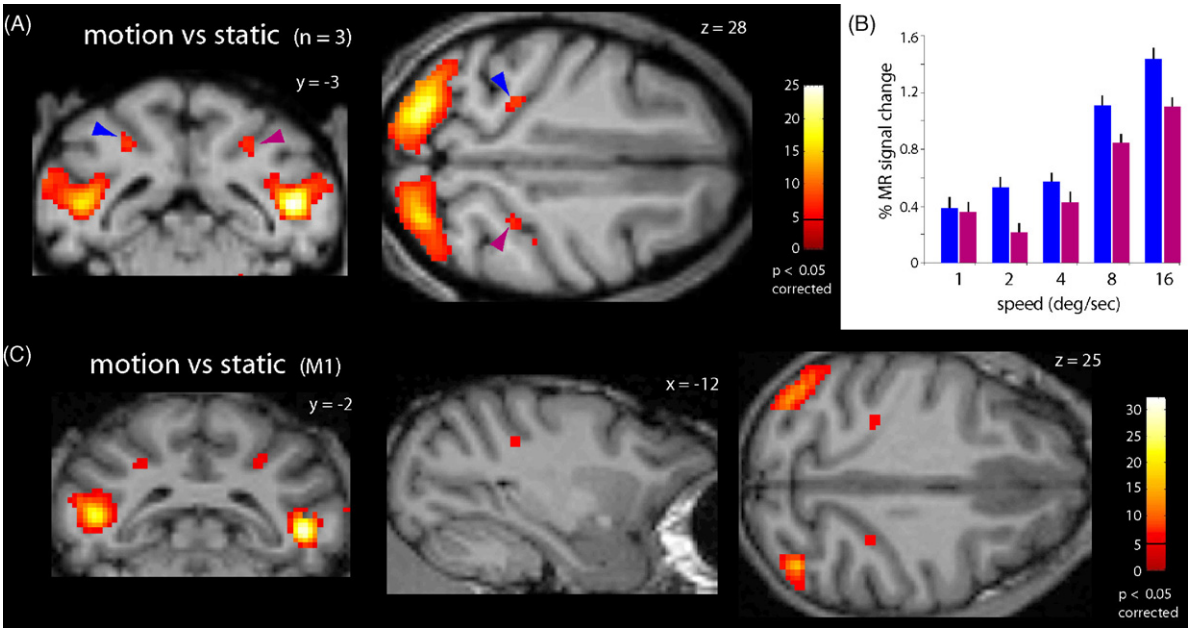

Fig. 3. Motion sensitive region in monkey IPS. (A) SPMs plotting voxels significantly ($P < 0.05$ corrected for multiple comparisons) more active when monkeys (M1, M4, M5) as a group view translating random textured patterns compared to their static counterpart, superimposed on coronal and horizontal sections at level indicated. (B) Activity profiles plotting % MR signal change compared to static baseline for five speeds in left (blue) and right (purple) VIP, identified as the seven voxels neighboring the local maxima in (A). (C) SPM plotting voxels significantly more active for moving ($16\,s^{-1}$) than stationary random texture patterns (diameter 4°, single subject M1), superimposed on coronal, sagittal and horizontal sections at levels indicated.

tasks. Critically, the visual input was the same in all conditions, only the task given to the subjects differed. This experiment revealed two IPS regions, both in the dorsal segment, that were involved in 3D shape judgments more than in the other tasks. The more posterior of the two included DIPSM, the more anterior one was located in front of DIPSA, but extended caudally into DIPSA. While the posterior region was involved only in 3D shape judgments, the anterior one was also involved in 3D motion judgments. This latter region was located near the putative homologue of monkey AIP (Binkofski et al., 1999; Grefkes et al., 2002). This is consistent with the observation that for grasping moving objects, both the 3D shape and trajectory in space are important visual parameters.

3.3. Monkey IPS: further observations on motion sensitivity

In the initial study (Vanduffel et al., 2001), a single motion sensitive region was mapped in the monkey IPS using translating random dots: VIP. This result was confirmed in the present study by testing translating random dots over a range of speeds (1–16°/s). Contrasting all five motion conditions to a stationary dot control yielded a single significant activation site corresponding to the earlier defined VIP region. This was true (Fig. 3A) for the group analysis of all three monkeys (M1, M4 and M5), and in each individual subject, as illustrated for M1 in Fig. 3C and for M5 in Fig. 4. In monkey M1 the motion activation was closer to the fundus of the sulcus (see also Fig. 2 in Vanduffel et al. (2001)) than in monkey M5. Thus in some monkeys the motion activation may include part of LIPv (Lewis & Van Essen 2000). The activity profile plotting the % change in MR signal compared to fixation for the different conditions indicates that MR activity increases monotonically with speed up to the maximum (Fig. 3B). Thus the present study confirmed the important difference between human and macaque IPS with respect to motion sensitivity (Orban et al., 2003). It also suggests that the VIP defined here on the basis of its motion sensitivity, as assessed by fMRI, may be more restrictive, and more localized on the lateral bank than the definition used in single cell studies which includes criteria of multimodality (Bremmer, Duhamel, Ben Hamed, & Graf, 2002a; Bremmer, Klam, Duhamel, Ben Hamed, & Graf, 2002b).

A further difference between these human and monkey IPS regions was revealed by the testing of 3D SFM. In the Vanduffel et al. (2002) study we tested three monkeys (M1, M3 and M4) using random lines angled 90° with respect to each other, as described in the last control experiment of Orban et al. (1999). Two of these monkeys (M1, M3) and two additional ones (M5 and M11) were subsequently tested with a slightly different random line pattern in which the angles between the lines could have any value, as in the main experiment of Orban et al. (1999). This subsequent testing failed to reveal any significant activation in the subtraction 3D–2D shape in monkeys M1 and M3, in agreement with the earlier report of Vanduffel et al. (2002). The two other monkeys, however, exhibited two significant activation sites in the lateral bank of the IPS (Fig. 4): one anterior, slightly more dorsal and rostral than VIP, and the other 7 mm more posterior. The relationship of these two activation sites to VIP identified by its motion sensitivity and to LIP and pIPS, as identified by their shape sensitivity (Denys et al., 2004a) is illustrated for monkey M5 in Fig. 4. The anterior 3D SFM activation site is located dorsally with respect to VIP, more clearly so on the coronal sections (top) than on the flatmaps (bottom), which

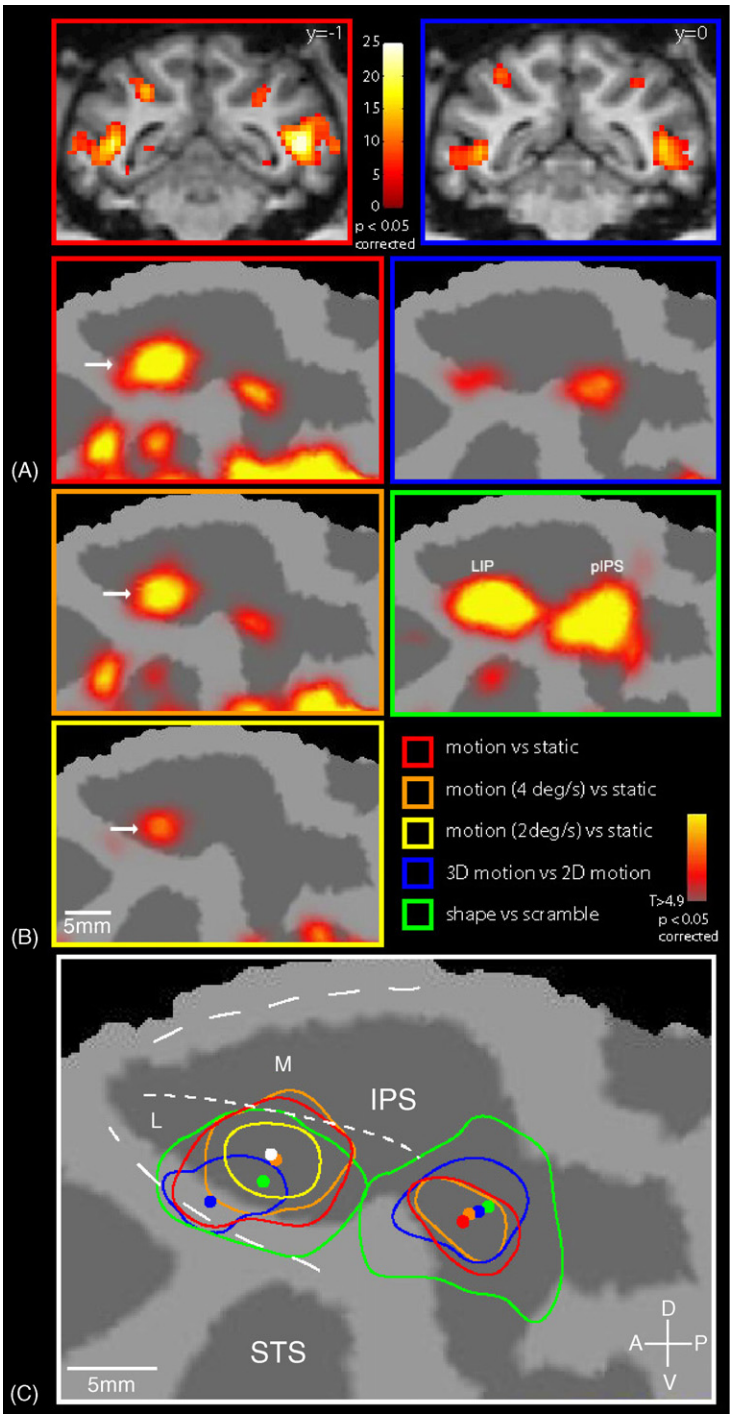

Fig. 4. 3D SFM sensitive regions in monkey M5 compared to motion sensitive region VIP and shape sensitive regions LIP and pIPS. SPMs plotting voxels significantly ($P < 0.05$ corrected) more active in the contrasts indicated by the color label of frames (see inset) superimposed on coronal sections (A) and on flat maps of left IPS (B). (C) schematic left IPS with outline of activated regions (redrawn from B) and local maxima (same color conventions as in A and B). In (B) arrow points to VIP defined by its motion activation. In (C) stippled lines indicate edges of IPS, underestimated by the curvature measure used to identify sulci in Freesurfer, L and M lateral and medial banks of IPS. The posterior 3D SFM region overlaps with pIPS, the anterior one is slightly lateral (on flatmap, dorsal in brain) from LIP, which itself is lateral (dorsal) from VIP. Notice that overlap is smaller on the sections (A) than on the flatmaps (B and C) which include deformation of the cortical sheet. For overlap between LIP and VIP see also Fig. 9 in Denys et al. (2004a,b).

contain a fair amount of distortion. This anterior site was also located somewhat more dorsal than LIP (defined by its shape sensitivity), and might correspond to LIPd of Lewis and Van Essen (2000). The posterior site overlapped with pIPS, which in this monkey also responded weakly to motion.

Despite this variability between monkeys (see also Tsao & Tootell, 2004, and Tsao et al., 2003), the new results reported here amply confirm our initial observation that human IPS is much more engaged by motion processing than is its monkey counterpart. Simple translating stimuli activate four human IPS

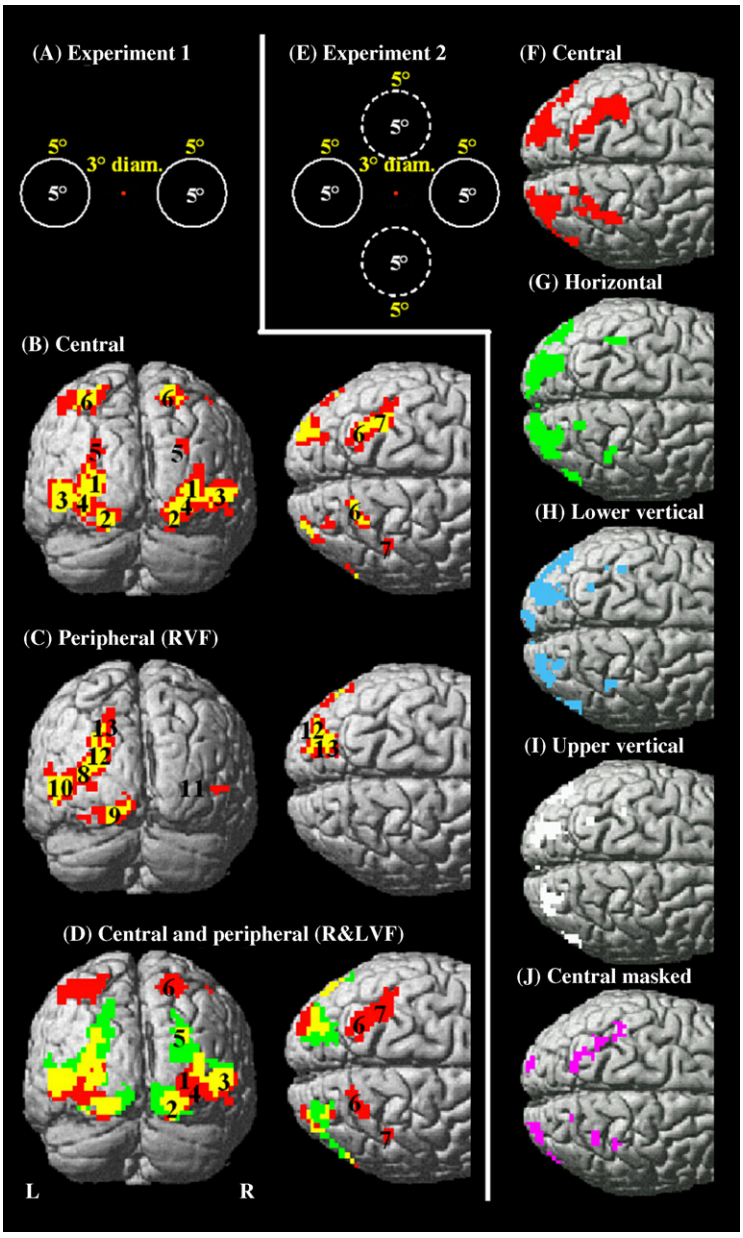

Fig. 5. Central and peripheral motion processing in humans. (A) Stimulus configuration in experiment 1: RTP was positioned either centrally or 5° into left and right visual field (red dot indicates fixation point). (B and C) Statistical parametric maps (SPMs) showing voxels (FWHH for group, 6 mm and for single subjects, 3 mm) significant (yellow: $P<0.0001$ uncorrected for multiple comparisons, corresponding to a false discovery rate of less than 5% false positives; red: $P<0.001$ uncorrected) in the group random-effects analysis (experiment 1, $n=16$) for the subtraction moving minus stationary conditions for the centrally (B) and peripherally (right visual field) (C) positioned stimulus, rendered on the posterior and superior views of the standard human brain. Further statistical testing revealed that he interaction between type of stimulus (motion, stationary) and location (center, periphery) was significant (random effects analysis) in DIPSA ($Z=3.12$, $P<0.001$ uncorrected and $Z=3.58$, $P<0.001$ uncorrected for right and left, respectively), DIPSM ($Z=3.58$, $P<0.001$ uncorrected and $Z=4.35$, $P<0.0001$ uncorrected for right and left, respectively) and weakly in POIPS ($Z=2.69$, $P<0.01$ uncorrected and $Z=2.24$, $P<0.01$ uncorrected for right and left, respectively). (D) Overlap of voxels ($p<0.001$ uncorrected; yellow) in the group random-effects analysis for the subtraction moving minus stationary conditions for the centrally (red) and peripherally (right and left visual field; green) positioned stimulus (experiment 1), rendered on the posterior and superior views of the standard human brain. (E) Stimulus configuration in experiment 2: RTP was positioned centrally or at 5° eccentricity on upper or lower vertical or horizontal meridian. (F–I) SPMs showing voxels significant ($P<0.05$ corrected) in experiment 2 ($n=3$) for the subtraction moving minus stationary conditions for the stimuli positioned in the central visual field (F, red), peripherally left and right on the horizontal meridian (G, green), and on the lower (H, blue) and upper vertical meridian (I, white), rendered on the superior view of the standard human brain (posterior part). (J) SPM showing voxels that are active only in the central condition (obtained by exclusive masking of the subtraction in F with those in G–I). The opposite procedure, subtractions (G)–(I) masked by that in (F), yielded no active voxels. R, right; L, left; VF, visual field. White and yellow numbers in A and E indicate eccentricity and diameter (diameter), respectively. Numbers in (B)–(D) correspond to the activation sites listed in Table 2.

regions compared to the single VIP region in the monkey. The same four human IPS regions are also activated by 3D SFM stimuli, which in monkeys drive either no IPS region (3/5 subjects) or 2 regions (2/5 subjects).

3.4. Human IPS: central/peripheral organization and shape sensitivity

In the control experiments of the Claeys et al. (2003) study we observed that, somewhat counter-intuitively the motion response of the IPS regions differed for stimuli presented in the center and 5° into the periphery of the visual field. Since this might provide a means to further differentiate the IPS motion sensitive regions, we investigated this issue in five experiments. In experiment 1 we compared motion responses (defined as MR signal change induced by motion compared to that induced by a static control stimulus) evoked by random dot patterns presented either in the center of the visual field or 5° into the left or right visual field (Fig. 5A). A random effects analysis yielded significant ($P < 0.0001$ uncorrected) motion activation of DIPSM and DIPSA by the central stimulus and a significant motion activation of POIPS by the peripheral stimuli (Fig. 5B and C, Table 2). Other regions including hMT/V5+ and VIPS were activated by both stimuli. In experiment 2 we generalized this finding to peripheral stimuli positioned on the horizontal, and on the upper and lower vertical meridians (VM). The motion activation of DIPSA and DIPSM by the central stimulus was much more extensive than that by any of the peripheral stimuli (compare Fig. 5F with G–I). This was confirmed by exclusive masking of the central response by all three peripheral responses (Fig. 5J).

In a third experiment, we explored the motion response to multiple positions on the HM (Fig. 6). Since the most conspicuous change in the first two experiments (Fig. 5) was the extent of activation, we expressed the motion response by its extent, defined as the number of significant voxels, specifically responding to motion at one of three eccentricities. The resulting curve (Fig. 6) confirms that DIPSA and DIPSM indeed represent only the central visual field, POIPS only peripheral positions, while VIPS exhibits a bimodal curve. It is worth noting that in V1 the number of motion sensitive voxels did not vary with eccentricity indicating that the changes in stimulus sizes compensated for the difference in magnification in this area, in agreement with the values derived for human V1 by Sereno et al. (1995). This means that DIPSA and DIPSM over represent central vision to a larger degree than V1! To control for possible effects of attention and interactions between hemifields, we carried out a fourth experiment with stimuli restricted to one field while the subjects detected a dimming in a portion of the stimulus (Fig. 7). Results were only qualitatively similar to those of experiment 3. Using the V1 activation as a reference to compare experiments 3 and 4 quantitatively, DIPSA, DIPSM and POIPS activations are less extensive, while those of VIPS and V3A are more extensive in experiment 4 than in 3.These quantitative changes induced by the attention task of experiment 4 are consistent with earlier imaging and single cell studies (Bisley & Goldberg, 2003; Constantinidis & Steinmetz, 2001; Powell & Goldberg, 2000; Tootell, Mendola, Hadjikhani, Liu, & Dale, 1998; Vandenberghe et al., 2001) leaving the qualitative effect of eccentricity, which was indeed very similar in the experiments 3 and 4. Furthermore, the last experiment suggests that the effects of attention differ between VIPS and the other three motion sensitive regions in human IPS (see below).

All these experiments were performed on a 1.5 T magnet and full retinotopic details, such as those of V7 (Tootell et al., 1998), could not be observed. Very recently we have switched to a 3 T magnet and in a fifth experiment we mapped response to central and peripheral positions along the different meridians with

Table 2
Activation sites involved in central or peripheral lower-order visual motion processing-

Region	Right VF				Left VF			
	x	*y*	*z*	*Z*-score	*x*	*y*	*z*	*Z*-score
(A) Central								
1. hV3A	−30	−93	3	5.15	30	−93	3	4.83
2. LG	−21	−93	−12	5.31	21	−93	−6	5.06
3. hMT/V5+	−48	−75	−3	5.07	51	−72	0	4.79
4. LOS	−39	−78	−3	4.31	36	−81	−3	4.19
5. VIPS	−27	−84	30	3.90*	30	−78	30	3.62*
6. DIPSM	−30	−60	57	4.43	24	−60	57	4.33
7. DIPSA	−36	−51	63	4.87	42	−45	57	3.62*
(B) Peripheral								
8. hV3A	−33	−87	12	4.83	24	−84	18	4.49
9. LG	−15	−84	−12	5.02	21	−81	−18	4.88
10. contra hMT/V5+	−51	−75	−3	4.55	48	−75	−3	5.35
11. ipsi hMT/V5+	48	−66	3	3.54*	−45	−72	3	3.90*
12. VIPS	−24	−81	24	4.79	27	−81	33	4.20
13. POIPS	−18	−81	45	3.98	21	−78	48	3.12*

Contra, contralateral; DIPSA, dorsal intraparietal sulcus anterior; DIPSM, dorsal intraparietal sulcus medial; hMT/V5+, human middle temporal complex; hV3A, human visual area 3A; ipsi, ipsilateral; LG, lingual gyrus; LOS, lateral occipital sulcus; POIPS, parieto-occipital intraparietal sulcus; VF, visual field; VIPS, ventral intraparietal sulcus.

* All activation sites in random-effects analysis at $P_{uncorrected} < 0.0001$ and at $P_{uncorrected} < 0.001$.

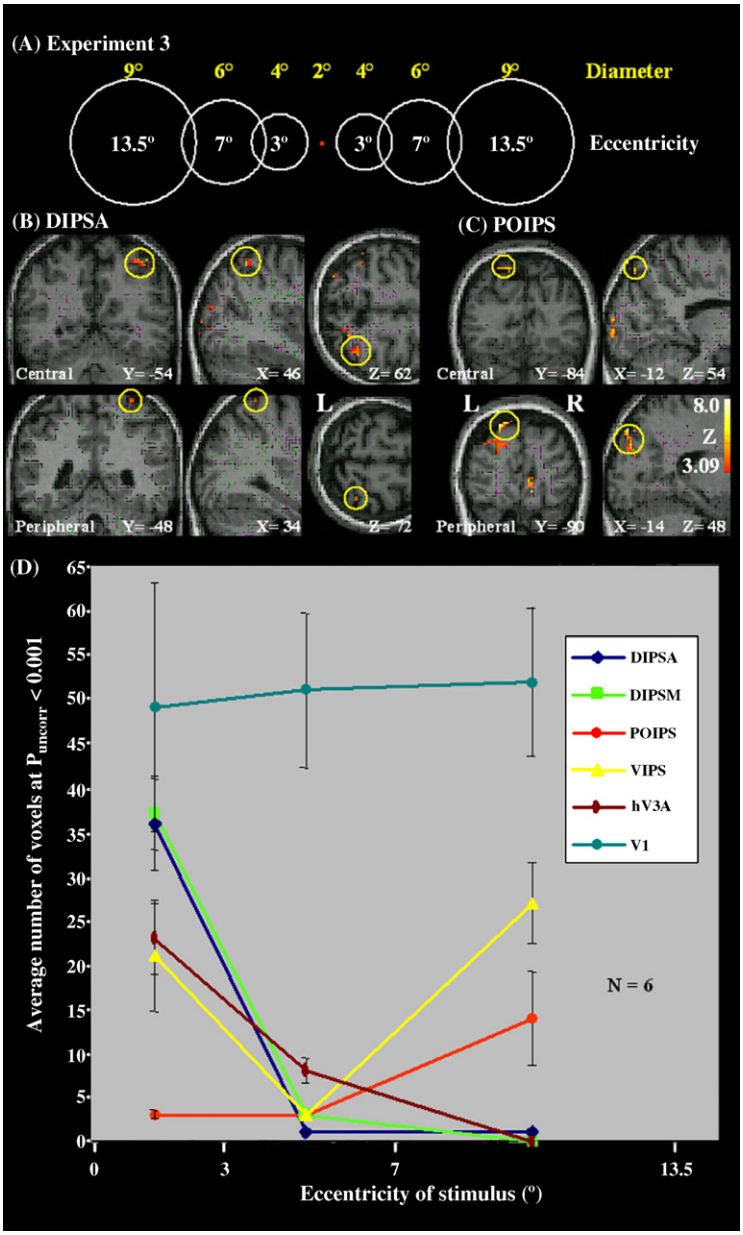

Fig. 6. Eccentricities represented in the IPS motion regions. (A) Stimulus configuration in experiment 3: RTP was presented centrally or at 3 eccentricities (3°, 7°, 13.5°) into left and right visual field. Stimulus diameter was adapted to eccentricity. (B and C) SPMs showing the activation in right DIPSA (B) and left POIPS (C) (both outlined in yellow), in a single subject ($P < 0.001$ uncorrected for multiple comparisons) for the subtraction moving minus stationary stimuli (averaged over all four eccentricities) exclusively masked with the same subtraction for the two most peripheral stimuli (central activation site at 1.5° eccentricity, upper panels) or the two most central stimuli (peripheral activation site at 10.25° eccentricity, lower panels). The SPMs are projected onto individual coronal, sagittal and transversal sections. The Talairach coordinates of the activation sites are indicated by *X*, *Y*, *Z* values. The color bar indicates *Z*-scores. (D) The number of active voxels ($P < 0.001$ uncorrected, exclusive masking) for each motion processing region (see inset) is averaged across the six hemispheres of the subjects that participated in experiment 3, and is plotted as a function of eccentricity of the stimuli. In order to ensure that the voxels were activated only by a given eccentricity rather than by that eccentricity and possibly others as well, we used an exclusive masking procedure, in which the motion response (% change in motion condition compared to stationary condition) to all four positions was exclusively masked by that to two positions: either the two central positions, the two most peripheral ones or the two most extreme. The masking with two rather than three positions was performed to allow for overlap between the representations of neighboring positions in the visual field. This procedure yielded an estimate of the number of voxels specifically responding to motion at one of three eccentricities (intermediate between those of the stimulus positions). Error bars represent S.E.M. For other conventions and abbreviations see Fig. 5.

a variety of stimuli: flickering black and white or colored dots, moving random dots, moving random lines and static figures. These recent results have confirmed the overrepresentation of central vision in VIPS, DIPSM and DIPSA (Fig. 8). In this new setting the location of the central field representation in hV3A, shared with V7, as described by the Stanford group (Wandell, Brewer, & Dougherty, 2005), has also become clearer. Finally VIPS seems to be located directly next to the pair hV3A/V7, an arrangement also suggested by Wade, Brewer, Rieger, and Wandell (2002). This last experiment has provided further evidence of specialization in the four motion sensitive IPS regions: the central representations become gradually more specialized

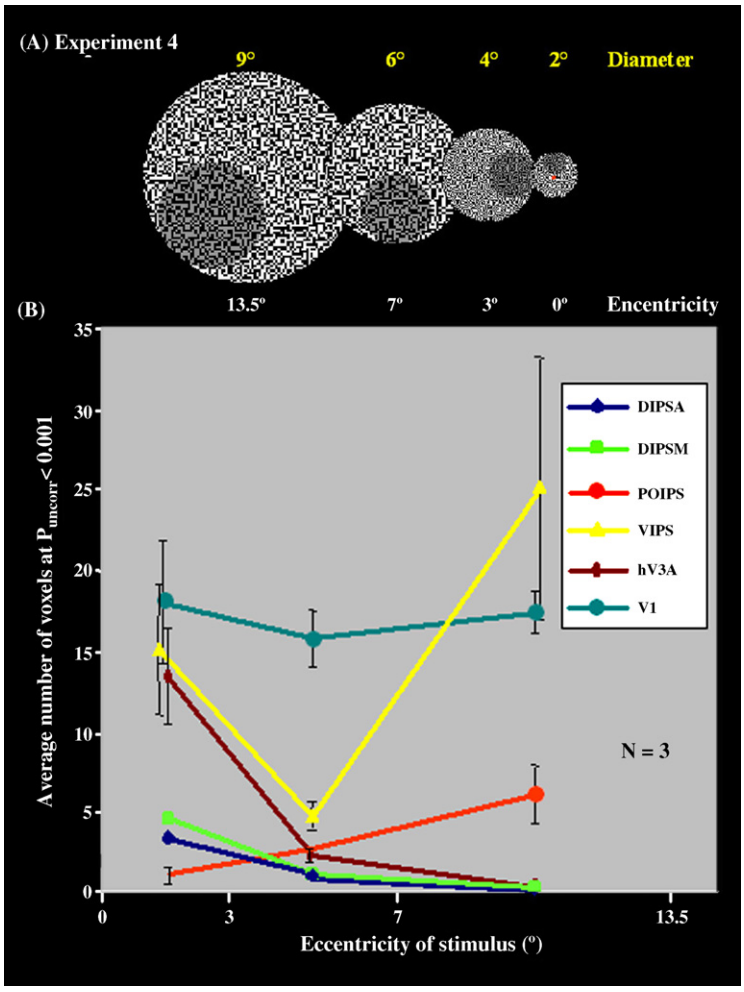

Fig. 7. Eccentricities represented in IPS regions under active conditions. (A) Stimulus configuration in experiment 4: RTP was presented centrally or at three eccentricities in the left visual field. The pixel size was increased from 3 × 3 to 6 × 6 minarc in the two most peripheral stimuli. Also, a fixed size (25%) and randomly positioned portion of the stimulus dimmed for 200 ms at unpredictable times (three to six times per 30 s epoch). Subjects responded within 600 ms with their right index finger and were trained in this task for 1.5 h before scanning. (B) Average ($n = 3$) number of active voxels ($P < 0.001$ uncorrected, exclusive masking) for each motion processing region (see inset) of the right hemisphere plotted as a function of eccentricity in experiment 4. For other conventions see Figs. 5 and 6. Notice the similarity in slope of the V1 curves in this and the preceding figure: this indicates that the differences in texture grain in the stimuli of experiment 4 had little effect.

for motion stimuli as one moves from VIPS to DIPSM and finally DIPSA (Fig. 8 inset), in agreement with our earlier results (Denys et al., 2004a,b).

The last data sets to become available for comparison between the two primate species concern shape sensitivity. In a recent study (Denys et al., 2004a) we showed that four human IPS regions were involved in the processing of shape, reacting more to the presentation of intact than scrambled images of objects. One of the regions overlapped with VIPS, while the three other were located in close proximity (slightly lateral) to the POIPS, DIPSM and DIPSA. To avoid the proliferation of new region labels, we tentatively refer to these regions as POIPSs, DIPSMs and DIPSAs (Fig. 1B), the 's' standing for shape. In a subsequent study using a similar but different set of smaller shapes (Sawamura et al., 2005) no POIPSs activation was observed while the DIPSMs and DIPSAs activation was comparatively much stronger (Fig. 1C). In both studies extensive control experiments were performed to exclude the possibility that attention effects might explain the differences in response to intact and scrambled object images. These control experiments in which subject performed a demanding task in central vision (Vanduffel et al., 2001) have also indicated that the effects of the task differ between VIPS and the other IPS regions: while VIPS is hardly affected by the task, the activity in the three others is increased with the task, somewhat more for scrambled than for intact conditions (Fig. 9). The shape effect, however, remained significant in all regions (Denys et al., 2004a).

3.5. Monkey IPS: shape sensitivity and retinotopy

In the Denys et al. (2004a) study we compared shape sensitivity, as assessed by the effect of scrambling on greyscale images and drawings of objects, for humans and monkeys. Two shape sensitive regions were observed in monkey IPS (Fig. 10A). Our retinotopic mapping study of monkey visual regions (Fize et al., 2003) had revealed a central visual field representation in the lateral bank of IPS. Ben Hamed, Duhamel, Bremmer, and Graf (2001) had performed a detailed single cell study and mapped

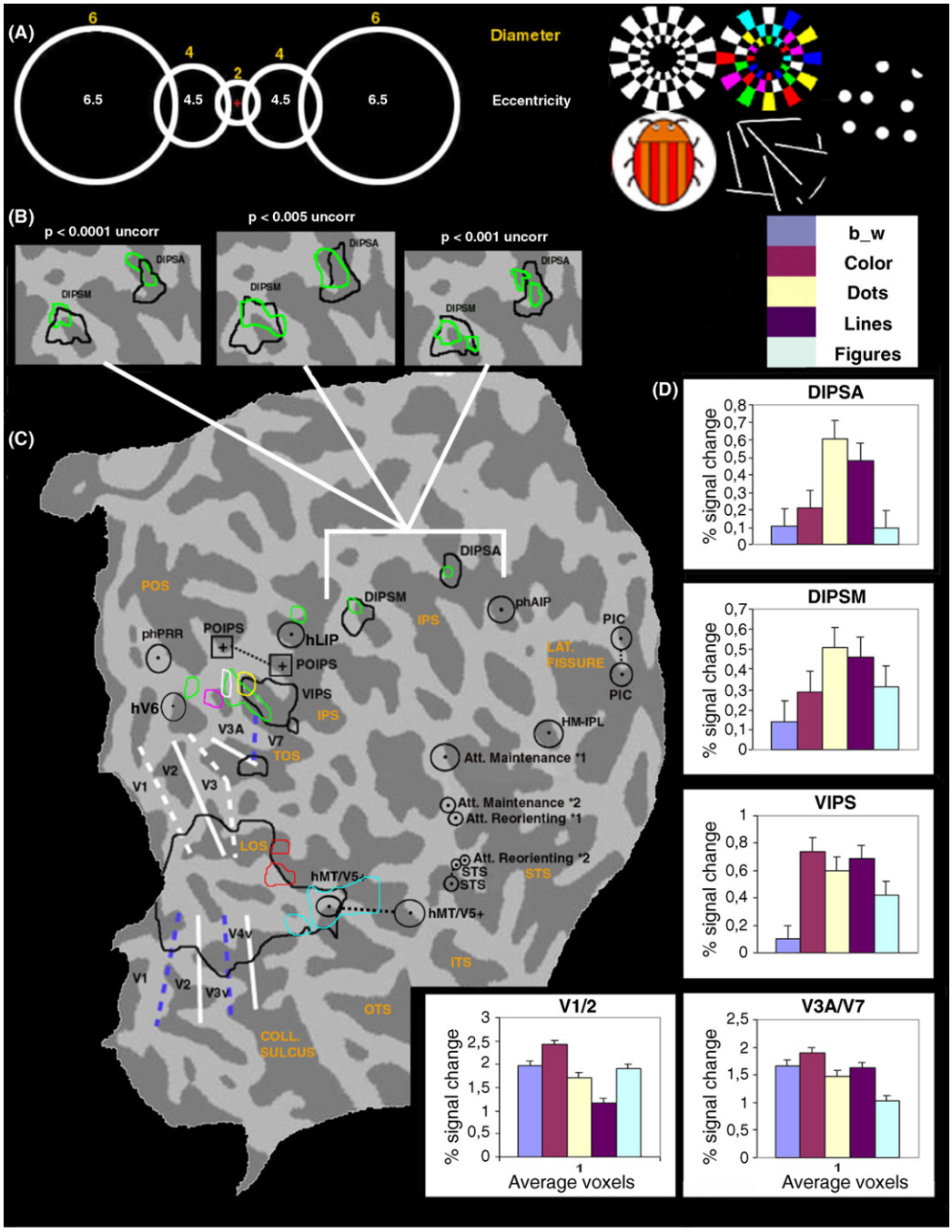

Fig. 8. Flatmap of human right hemisphere (single subject) with retinotopic regions and central visual field representations. (A) Stimuli: location (eccentricity), size (diameter) and schematic indication of five stimulus types: back and white and colored flickering checkerboards, moving random dots and lines, and figures. (B) Part of flatmaps containing central representations of DIPSM and DIPSA at different levels of significance indicated. (C) Flatmap of posterior part of right hemisphere with upper and lower vertical meridians (blue and white stippled lines) and horizontal meridian (while solid lines) and central representations (black solid lines), 4.5° and 6.5° eccentricity on horizontal meridian (green and white solid lines), 4.5° and 6.5° eccentricity on lower vertical meridian (yellow and pink lines), motion sensitive regions (blue and red outlines respectively). (D) activity profile plotting % MR signal change compared to fixation for the five types of central stimuli for five central visual field representations: that common to V1/V2, that common to V3A and V7, and the three IPS representations. Notice the increase in selectivity for motion along the IPS. In (C) the sulci are indicated in orange abbreviations, see Fig. 1, LOS: lateral occipital sulcus. The location of the fourth IPS region, POIPS, is estimated from its coordinates 25, −75, 45 (Orban et al., 2003) and 21, −78, 48 (Table 2) and is indicated by squares surrounding crosses. Location of motion sensitive regions (hMT/V5+ (51, −69, 3 and 54, −60, 0), STS (57, −48, 12 and 54, −51, 12), PIC (51, −30, 21 and 42, −33, 21)) and the higher order motion region in IPL (HM-IPL, 63, −36, 30) estimated from their Talairach coordinates in Orban et al. (2003), Claeys et al. (2003), Peuskens et al. (2004, 2005), location of putative human homologues of AIP (40, −42, 38, Binkofski et al., 1999; Grefkes et al., 2002) and PRR (1, −74, 38, Connolly et al., 2003) and human homologue of LIP (19, −63, 49, Koyama et al., 2004) and V6 (estimated from Dechent and Frahm (2003)), as well as regions involved in reorienting (53, −49, 30 and 57, −45, 12) and maintenance of attention (52, −51, 30 and 54, −60, 33) are indicated by circles surrounding dots. Notice that panel B indicates that changes in threshold, while increasing the absolute extent of activation (number of activated voxels) do not alter their relative sizes for different eccentricities, supporting the procedure used in Figs. 6 and 7.

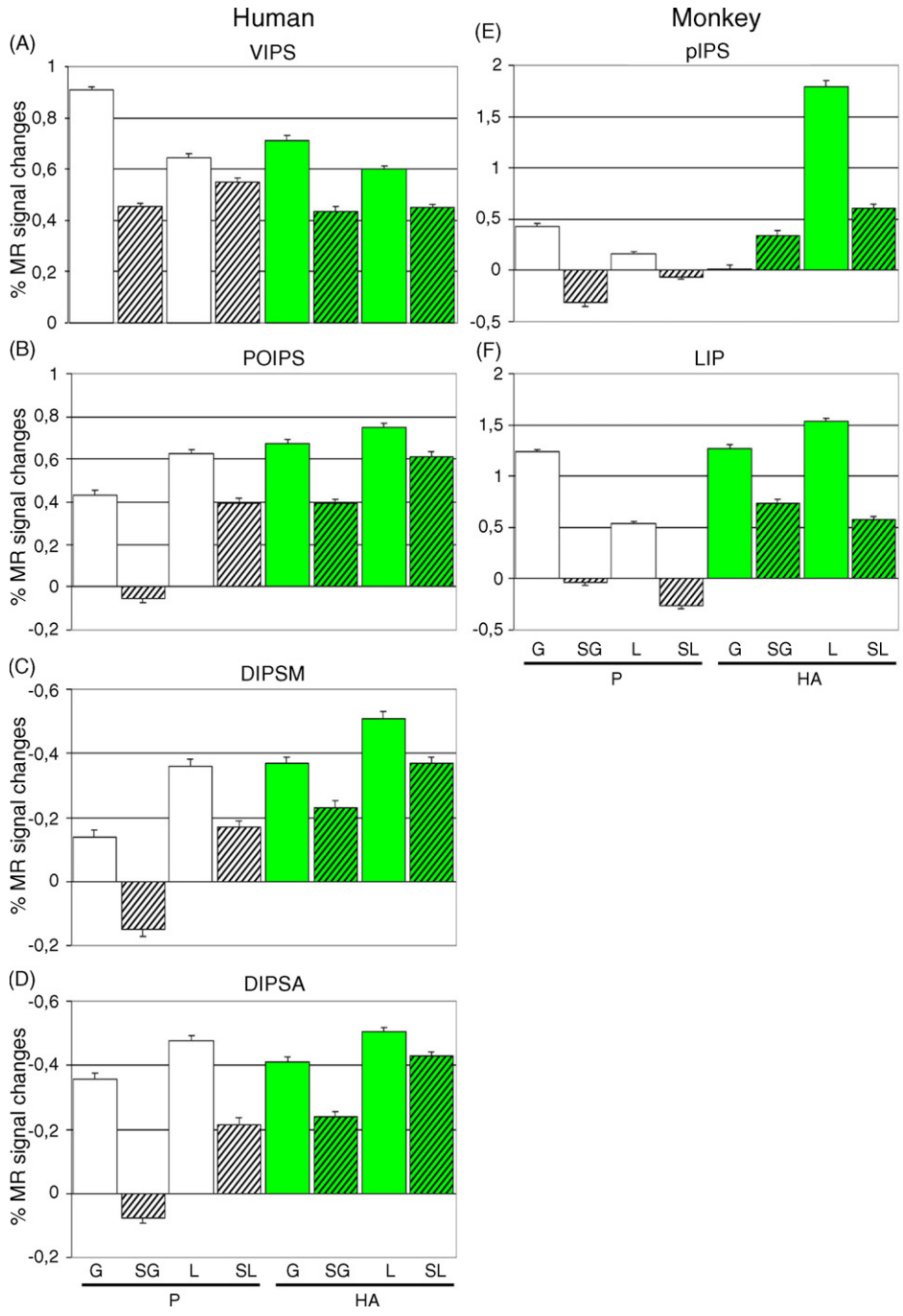

Fig. 9. Activity profiles plotting % MR signal change, compared to fixation, for intact greyscale images (G) and drawings (L) and their scrambled counterparts (SG and SL) of four human IPS regions (A–D) and two monkey IPS regions (E and F) when subjects are passive (white columns) or performing a difficult acuity task (green columns). From Denys et al. (2004a).

a central representation in the anterior part of LIP. This was the rationale for labeling the shape sensitive region located at that anterior level in IPS as LIP (Denys et al., 2004a). Single cell studies have also indicated that a fraction of LIP neurons are selective for shape (Sereno & Maunsell, 1998). The more posterior shape sensitive region, located near the IPS fundus was tentatively labeled pIPS as it did not clearly match any of the earlier descriptions (Van Essen, 2004). The subsequent Sawamura et al. (2005) study confirmed the shape sensitivity of the LIP region (Fig. 10B) but no shape effect was observed at the level of pIPS, in analogy with what has been observed for human POIPSs (Fig. 1C). As for human subjects, control experiments were performed in which the monkeys had to detect the unexpected change in the orientation of a small central bar (Vanduffel et al., 2001), while the shape stimuli were presented in the background. In both LIP and pIPS performing the task increased activation (relative to fixation baseline condition), again more in the scrambled than in the intact conditions (Fig. 9E and F). Furthermore, in pIPS the task effect was stronger for the drawings than the greyscale figures, probably reflecting an interaction

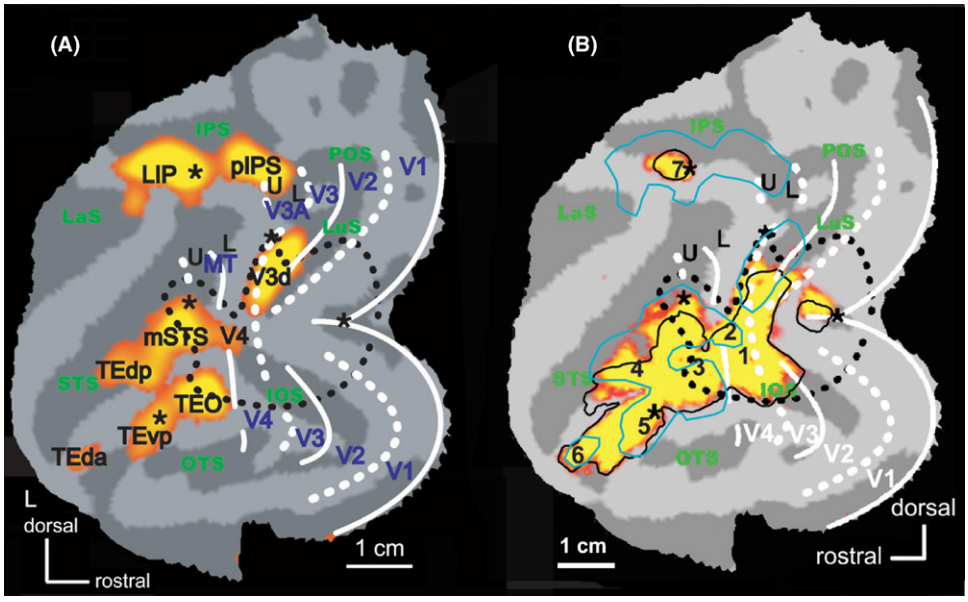

Fig. 10. Flatmaps of posterior part of left monkey hemisphere indicating shape sensitive regions. SPMs plotting voxels significantly more active ($P < 0.05$ corrected) for intact than scrambled images of objects (A) and for intact vs. phase scrambled small shapes (B). Same stimuli as in Fig. 1B and C. Data from Denys et al. (2004a,b) (A) and Sawamura et al. (2005). White solid and stippled lines: horizontal and vertical meridians, black dotted lines and stars: central representation. In (A) retinotopic regions are in blue, shape sensitive regions in black and sulci in green. In (B) sulci are in green, blue lines are the outlines of shape sensitive regions in (A) and numbers label local maxima of shape sensitivity. STS: superior temporal sulcus, OTS: occipito-temporal sulcus, IOS inferior occipital sulcus, LuS lumnate sulcus, POS: parieto-occipital sulcus, IPS: intraparietal sulcus, LaS lateral sulcus.

of task with the background stimuli: the little bar is more difficult to discriminate on a background of lines than grayscale figures. Thus shape sensitivity also reveals differences between the two species: three or four shape sensitive regions, depending on the stimuli, in humans versus one or two regions in the monkey.

Finally, subsequent experiments in which the Fize et al. (2003) data were reanalyzed with a new template and additional monkeys were mapped confirmed the representation of central visual field at the level of the anterior third of the lateral bank of IPS. This group (M3, M5, M11) study also revealed that the part of IPS posterior to this central representation is devoted to peripheral vision. Thus monkey IPS contains one representation of central vision (anterior LIP), human IPS three (VIPS, DIPSM and DIPSA).

4. Discussion

4.1. Pittfalls of human–monkey fMRI comparisons

Studies in which BOLD and MION measurements are compared in the same subjects have shown that the use of the contrast agent improved the contrast-noise ratio (by approximately five-fold) compared to blood oxygenation level-dependent (BOLD) measurements (Leite et al., 2002; Vanduffel et al., 2001). Because the MR signals obtained with MION and BOLD show a different relationship with vessel diameter, MION MR signals, unlike BOLD are more confined to the parenchym than to the superficial draining veins. This feature improves the resolution of the SPM statistical landscape and allows better detection of separate local maxima (see Fig. 3 in Vanduffel et al. (2001)). A third advantage of MION is the high contrast of the functional raw images which favors the registration of functional and anatomical images (Nelissen, Luppino, Vanduffel, Rizzolatti, & Orban, 2005). The smaller voxels size used in the monkey compared to human fMRI is offset partially by the greater sensitivity of MION measurements, hence the signal changes in homologous areas such as V1 remain stronger in the monkey (Denys et al., 2004b). The strength of the MION signals is also the rationale for using fewer monkey than human subjects in a given study. There are several additional differences between humans and monkeys in the MR measurement and postprocessing, that go beyond the scope of the present review, but are detailed in Orban et al. (2004).

The stimuli used in the same species are generally extremely similar as we compensate for the difference in the distance to the screen. Monkey subjects like humans are awake and possible differences in attention are minimized by the use of the control task.

4.2. The relationship between monkey and human IPS: a hypothesis

4.2.1. Difficulties inherent to inter-species comparisons

Before the advent of monkey fMRI a number of human regions have been proposed as homologues of monkey cortical areas, based on the single cell properties in these areas (for review of Culham et al., this issue, Grefkes & Fink 2005). This is a very difficult enterprise for several reasons. First it is difficult to predict the magnitude of the fMRI signal, tracking the average activity of millions of neurons, on the basis of the selectivity of a few hundred neurons recorded in a cortical area. Furthermore, imaging requires a control condition, which

determines the results as much as the experimental condition and which usually has not been investigated in the single cell studies. Finally, this extrapolation from single cell studies in monkeys to human imaging, assumes that no additional monkey cortical area has the same characteristics, so that these can uniquely identify a human counterpart. The identification of human MT/V5+ (Dupont, Orban, De Bruyn, Verbruggen, & Mortelmans, 1994; Tootell et al., 1995; Zeki et al., 1991) is the most successful example of this strategy to date, as it is generally accepted in the literature. But even in this case the identification has actually failed so far at the areal level, since there is general agreement that the motion activation site in human inferior temporal sulcus (ITS), referred to as hMT/V5+, corresponds to the monkey MT/V5 *complex*, which includes at least four areas (MT/V5, MSTd, MSTv, FST). Thus the homology is established at the level of the complex, not at the level of the individual areas (Dukelow et al., 2001; Huk, Dougherty, & Heeger, 2002), a situation that probably will occur frequently (Orban et al., 2004). Other attempts have been less successful than MT/V5: the homologue of V4 is in debate (Orban et al., 2004; Wandell et al., 2005) and the identification of human FEF has been long contested (Tehovnik, Sommer, Chou, Slocum, & Schiller, 2000). This latter debate has recently been settled by a parallel fMRI study in humans and awake monkeys (Koyama et al., 2004). Clearly such parallel studies are the only way forward since they remove at least one unknown: how to translate the single cell properties observed in a cortical area into an fMRI signature. They also address to some extent the issue of the uniqueness of the fMRI signature.

4.2.2. Human homologue of LIP?

We believe that the data reviewed here, together with the recent study of Koyama et al. (2004) and Baker, Patel, Corbetta, and Snyder (2005), allow us to identify the human homologue of monkey LIP. Before doing so we must return to the question of the fMRI signature of monkey LIP. In many neurophysiological and anatomical studies (Lewis & Van Essen, 2000; Mazzoni, Bracewell, Barash, & Andersen, 1996) LIP is rather extended in its anterior-posterior dimension, exceeding the distance of 7 mm between what we have referred to as 'LIP' and pIPS in the Denys et al. (2004a) study. We therefore propose that in fact both 'LIP' and pIPS observed in the fMRI shape sensitivity tests (Fig. 10A) are part of LIP complex as defined in the invasive studies. The term 'LIP complex' may well be in order since our fMRI suggests a rostro-caudal division ('LIP' and pIPS), while anatomical studies have suggested a dorso-ventral division (LIPd and LIPv, Lewis & Van Essen, 2000). This identification of the LIP complex is supported by our recent observation that both 'LIP' and pIPS are activated by saccades compared to a visual control (Wardak, Vanduffel, & Orban, 2005). Koyama et al. (2004) obtained the strongest eye-movement-related activation with clear contraversive selectivity in dorsal LIP of the monkey and in a human region labeled post SPL. This latter region, defined by its coordinates (x, y, z) is projected onto the flat map of Fig. 8 and labeled hLIP. The Koyama et al. (2004) observation as such is insufficient to unambiguously identify the LIP homologue since in that study several human and monkey regions in the neighborhood of LIPd and post SPL had similar properties. The hLIP of Koyama et al. (2004), however, lies just caudal to DIPSM (and DIPSMs), the central representation of which matches that of monkey 'LIP' (Fig. 10A). It also lies just rostral to POIPS and its shape sensitive counterpart, POIPSs (Fig. 8). The latter shares with pIPS a shape sensitivity which disappears for the stimuli used in the Sawamura et al. (2005) study (compare Figs. 1B and C with 10A and B). Thus these three observations together suggest that the cortex comprised between POIPS(s) and DIPSM(s) is the human homologue of the monkey LIP complex. This fits with earlier suggestions by Muri et al. (1996), Sereno, Pitzalis, and Martinez (2001) and Simon et al. (2002). The medio-lateral separation between DIPSM and DIPSMs may then correspond to the distinction between LIP(d) and the more ventral LIPv or VIP.

4.2.3. Putative homologues of AIP and PRR?

Fig. 8 also shows two other putative homologues of monkey regions: phAIP and phPRR. Since these two homologies are based only on indirect evidence, without the benefit of combined fMRI experiments in the two species, this attribution is even more tentative than that of hLIP, hence the use of the label 'putative homologue'. The location of phAIP is based on the coordinates of Grefkes et al. (2002) and Binkofski et al. (1999) and has been replicated in a series of studies using visually guided grasping and grasping approximations (Culham, 2004; Culham et al., 2003; Frey, Vinton, Norlund, & Grafton, 2005; Simon et al., 2002). Its multisensory convergence (visuo-tactile) has also been reported by Macaluso, Eimer, Frith, and Driver (2003), but it is not clear whether or not it supports the identification as phAIP (Behrmann et al., 2004). The phPRR is based on the coordinates of Connolly et al. (2003). Both regions are in the appropriate location relative to hLIP, with phAIP rostral from hLIP and phPRR caudal and medial. This was not the case for what has been suggested as phVIP by Bremmer et al. (2001). If we accept the phAIP location (Fig. 8), it implies that there is a much greater distance between the human homologues of AIP and LIP than between the original regions in the monkey. This would indicate that new cortical regions have evolved in the interval between DIPSM and phAIP, with DIPSA being one of them. PRR includes V6A (Andersen & Buneo, 2002), and the human homologue of V6, neighboring V6A, has tentatively been located dorsally to V3 (Dechent & Frahm, 2003; Pitzalis et al., 2004). Thus most human homologues of the posterior IPS regions in the monkey have been at least tentatively identified.

4.2.4. Putative homologue of CIP?

One notable exception is the stereo selective region CIP identified in the single cell studies of the Sakata group (Taira, Tsutsui, Jiang, Yara, & Sakata, 2000; Tsutsui, Sakata, Naganuma, & Taira, 2002). The recent Tsao et al. (2003) study addresses this question. CIP is located in the posterior part of the lateral bank of monkey IPS. Either it is considered to be located behind the LIP complex (Tsutsui et al., 2002) in which case it is sometimes referred to as the LOP zone (Lewis & Van Essen, 2000) or alternatively it is seen as overlapping with the posterior part of this complex, as suggested by comparing the location of the units and

pIPS on coronal sections (this study). Tsao et al. (2003) obtained activation by stereo checkerboard stimuli in a posterior region of monkey IPS, labeled CIPS, which they considered equivalent to the CIP region of single cell studies. In humans they identified a region in the occipital part of IPS, dorsal to V7, with properties similar to CIPS, which they refer to as CPDR. Thus the motion sensitive VIPS region might correspond to CPDR and hence be the homologue of monkey CIP. However, unlike VIPS in humans, it is unclear whether or not CIP in the monkey is directly adjacent to V3A. A possible alternative scheme is that CPDR, which was rather extensive (Fig. 4 in Tsao et al. (2003)), actually corresponds to both VIPS and POIPS. In that scheme CIP would actually largely overlap with pIPS in the monkey. VIPS would then be the homologue of the small region in the posterior IPS of the monkey positioned between CIP/pIPS and V3a. This part of monkey IPS has a typical occipital architectonic pattern (Luppino, personal communication) and indeed VIPS has a number of characteristics that set it apart from the three other IPS motion sensitive regions, which correspond more to typical parietal regions: (1) Its activity is enhanced by attention to contralateral targets, as in extrastriate regions (Vandenberghe et al., in press and Fig. 7). (2) We have seen that the effect of the acuity task in VIPS differed from that in the other three IPS motion sensitive regions (Fig. 9). VIPS would then belong to this set of dorsal occipital regions that includes V3A, V6, MT/V5 (and possibly V7). These areas are located both geographically and hierarchically between the early retinotopic regions (V1–4) and the parietal regions, and act as gateways to the parietal regions. Like the early retinotopic regions, and the more ventral extrastriate regions, they are modulated by spatial attention.

4.3. The PPC ProtoMap as a principle for organizing data interpretation: locating attention effects

Once a proto-map of human PPC is available it becomes a helpful guide for interpretation of the human imaging data. It provides a reference for the localization of the activation sites and may help in interpreting the activation sites, because links with single cell studies can be established with some degree of certainty. To illustrate this we will use attention as an example and localize some of the dissociations described in Section 1. A first distinction is that between endogenous control of attention and reorienting to targets appearing at unattended locations (Corbetta et al., 2000). Endogenous control, including shifts of spatial and maintenance of up to 7 s, activates two sites included in the human homologue of the LIP complex (close to the hLIP in Fig. 8). Reorienting involves more ventral regions at the TPJ junction (IPL and STG), indicated as reorienting 1 and 2 in Fig. 8. A second distinction exists between shifts in spatial attention and maintenance of attention in a fixed position. According to Vandenberghe et al. (2001) shifts in attention activate the SPL, just medial of hLIP in Fig. 8. This fits the overlap between covert and overt shifts documented in this and a host of other studies (Beauchamp et al., 2001; Corbetta et al., 1998; Perry & Zeki, 2000). Subsequent studies have implicated this region not only in spatial shifts of attention but also in shifts of attention between objects and even between features (Yantis & Serences 2003). In the Vandenberghe et al. (2001) study, maintaining attention for 30 s activated much more ventral regions located in the angular gyrus of IPL (maintenance 1 and 2 in Fig. 8), caudal to the higher order motion region (HM-IPL, Claeys et al., 2003), and dorsal to the reorienting sites. Thus the PPC proto map allows one to report coherently the different attention effects.

4.4. New functional properties or new areas?

4.4.1. Posterior IPS

The schema presented above suggests that the part of human IPS posterior to DIPSM follows relatively closely the general primate plan, also present in the old world monkey. Yet even in this part of IPS functional properties differ between species. One possible origin of these functional differences is a change in the properties of the afferent areas. It is well established that V3A projects into the IPS (Nakamura et al., 2001). In humans this area acquires new properties, specifically motion, 3D SFM and shape sensitivity (Denys et al., 2004a; Vanduffel et al., 2001, 2002). It also seems to emphasize central vision more in humans than in the monkey (Wandell et al., 2005, present report). Thus the projection from V3A may then simply transmit these properties to its target regions, such as VIPS and DIPSM. Thus the motion sensitivity of DIPSM must not necessarily be interpreted as an indication that DIPSM derives from VIP, it may well derive from LIP and have acquired motion sensitivity from its afferents. It has recently been suggested that V6 and MT/V5 are the sources of two parallel pathways through monkey PPC (Rizzolatti & Matelli, 2003). We suggest that V3A plays a similar role, at least in humans, giving rise to multiple pathways through human PPC. The function of this ‘new’ pathway would be to inject motion signals related to the central visual field into the IPS.

4.4.2. Anterior IPS

On the other hand, the part of human IPS anterior to hLIP, but posterior to phAIP, seems to be evolutionarily new to a large degree, a conclusion also reached by Simon et al. (2002). It is thus likely that central representation in DIPSA originates from a duplication of the anterior part of LIP (or the posterior part of AIP). Therefore, the three central representations in human IPS would each have a different origin. That in DIPSM might correspond to that in anterior LIP of the monkey; that in VIPS might arise from the new properties of its afferents from hV3A, while that in DIPSA would have appeared by duplication of the central representation in monkey LIP/AIP. At present, this is only a hypothesis, but one that can be tested by further parallel imaging studies in humans and monkeys.

The large expanse of IPS devote to central vision is consistent with the increased use of tools in humans (Forsssberg, 1999), a change we initially suggested for the differences in motion and 3D SFDM sensitivity between human and monkey cortex (Vanduffel et al., 2002). Indeed it has been reported that in humans, manipulation is accompanied by systematic saccades, in such a way that the next target to be manipulated is fixated ahead of time (Johansson et al., 2001). This

fixation strategy provides a spatial reference point for hand movements and movements of objects in hand. Thus, during manipulation humans operate with a functional fovea that has been estimated to be 2.5° in diameter (Terao, Andersson, Flanagan, & Johansson, 2002), in good agreement with the part of the visual field over represented in human IPS. It is unlikely that this overrepresentation subserves eye-hand coordination in the classical sense, which is achieved by a common eye-centered reference frame used in LIP and PRR (Andersen & Buneo, 2002), controlling saccades and reaching, respectively. This computational strategy, realized in posterior IPS, is evolutionary old and common to monkeys and humans. On the other hand, the saccadic marking of targets in manipulation, together with the over-representation in human PPC might be seen as a means by which an eye-centered frame could also be used for manipulatory hand movements. But this eye-centered frame would have an expanded central representation which allows very detailed analysis of the object to be manipulated along many dimensions such as size, 3D orientation, 2D and 3D shape, etc. providing very sophisticated control of manipulation (Johansson et al., 2001). Furthermore, Andersen and Buneo (2002) have suggested that one can convert eye coordinates in a direct way to limb coordinates if the hand is visible. Such a scheme would be very helpful when both hands are used for manipulation, or by extension, for the use of a coordinate frame attached to a tool. Thus an eye centered coordinate frame would also be advantageous for manipulation of objects and tools. The present data and their interpretation suggest that this is implemented in anterior IPS and greatly enhanced in humans.

5. Conclusion

The PPC links vision to action and hence parietal areas may differ with regard to the visual features analyzed or the types of body movements controlled. An increased number of cortical parietal regions in humans may be devoted either to control a wider range of body movements or to provide a more detailed analysis of the visual input. The present results support at least the later interpretation and indicate the significance of moving images in the visual input to human PPC. This reflects the increased significance of moving objects or objects with moving parts typical of tool handing and fabrication.

Acknowledgements

The technical help of Y. Celis, A. Coeman, M. De Paep, W. Depuydt, C. Fransen, P. Kayenbergh, G. Meulemans, is kindly acknowledged. Supported by grants GOA 2005/18, IUAP P5/04, GSKE, FWO G 0151.04, EU project Neuro-IT-Net (IST-2001-35498). CW is supported by the Fyssen foundation. The authors are indebted to G. Rizzolatti, G. Luppino and S. Raiguel for helpful comments on an earlier version of the manuscript. The Laboratoire Guerbet (Roissy, France) provided the contrast agent (Sinerem®).

References

Andersen, R. A., Bracewell, R. M., Barash, S., Gnadt, J. W., & Fogassi, L. (1990). Eye position effects on visual, memory, and saccade-related activity in areas LIP and 7a of macaque. *Journal of Neuroscience*, *10*, 1176–1196.

Andersen, R. A., & Buneo, C. A. (2002). Intentional maps in posterior parietal cortex. *Annual Review of Neuroscience*, *25*, 189–220.

Assad, J. A. (2003). Neural coding of behavioral relevance in parietal cortex. *Current Opinion in Neurobiology*, *13*, 194–197.

Astafiev, S. V., Shulman, G. L., Stanley, C. M., Snyder, A. Z., Van Essen, D. C., & Corbetta, M. (2003). Functional organization of human intraparietal and frontal cortex for attending, looking, and pointing. *Journal of Neuroscience*, *23*, 4689–4699.

Baker, J. T., Patel, G. H., Corbetta, M., & Snyder L. H. (2005). Distribution of activity across the monkey cerebral cortical surface, thalamus and midbrain during rapid, visually guided saccades. Cerebral Cortex.

Batista, A. P., & Andersen, R. A. (2001). The parietal reach region codes the next planned movement in a sequential reach task. *Journal of Neurophysiology*, *85*, 539–544.

Beauchamp, M. S., Petit, L., Ellmore, T. M., Ingeholm, J., & Haxby, J. V. (2001). A parametric fMRI study of overt and covert shifts of visuospatial attention. *NeuroImage*, *14*, 310–321.

Behrmann, M., Geng, J. J., & Shomstein, S. (2004). Parietal cortex and attention. *Current Opinion in Neurobiology*, *14*, 212–217.

Ben Hamed, S., Duhamel, J. R., Bremmer, F., & Graf, W. (2001). Representation of the visual field in the lateral intraparietal area of macaque monkeys: A quantitative receptive field analysis. *Experimental Brain Research*, *140*, 127–144.

Binkofski, F., Buccino, G., Posse, S., Seitz, R. J., Rizzolatti, G., & Freund, H. J. (1999). A fronto-parietal circuit for object manipulation in man: Evidence from an fMRI study. *European Journal of Neuroscience*, *11*, 3276–3286.

Bisley, J. W., & Goldberg, M. E. (2003). Neuronal activity in the lateral intraparietal area and spatial attention. *Science*, *299*, 81–86.

Braddick, O. J., O'Brien, J. M. D., Wattam-Bell, J., Atkinson, J., & Turner, R. (2000). Form and motion coherence activate independent, but not dorsal/ventral segregated, networks in the human brain. *Current Biology*, *10*, 731–734.

Bradley, D. C., Chang, G. C., & Andersen, R. A. (1998). Encoding of three-dimensional structure-from-motion by primate area MT neurons. *Nature*, *392*, 714–717.

Bremmer, F., Duhamel, J. R., Ben Hamed, S., & Graf, W. (2002). Heading encoding in the macaque ventral intraparietal area (VIP). *European Journal of Neuroscience*, *16*, 1554–1568.

Bremmer, F., Klam, F., Duhamel, J. R., Ben Hamed, S., & Graf, W. (2002). Visual-vestibular interactive responses in the macaque ventral intraparietal area (VIP). *European Journal of Neuroscience*, *16*, 1569–1586.

Bremmer, F., Schlack, A., Jon Shah, N., Zafiris, O., Kubischik, M., Hoffmann, K.-P., et al. (2001). Polymodal motion processing in posterior parietal and premotor cortex: A human fMRI study strongly implies equivalencies between humans and monkeys. *Neuron*, *29*, 287–296.

Chef d'Hotel, C., Hermosillo, G., & Faugeras, O. (2002). Flows of diffeomorphism for multimodal image registration. *Proceedings of the IEEE International Symposium on Biomedical Imaging*, *7/8*, 21–28.

Choi, H.-J., Zilles, K., Mohlberg, H., Schleicher, A., Fink, G.R., & Amunts, K., et al. (in press). Cytoarchitectonic identification and probabilistic mapping of two distinct areas within the anterior ventral bank of the human intraparietal sulcus. *Journal of Comparative Neurology*.

Churchland, A. K., & Lisberger, S. G. (2005). Discharge properties of MST neurons that project to the frontal pursuit area in macaque monkeys. *Journal of Neurophysiology*, *94*, 1084–1090.

Claeys, K. G., Dupont, P., Cornette, L., Sunaert, S., Van Hecke, P., De Schutter, E., et al. (2004). Color discrimination involves ventral and dorsal stream visual areas. *Cerebral Cortex*, *14*, 803–822.

Claeys, K. G., Lindsey, D. T., De Schutter, E., & Orban, G. A. (2003). A higher order motion region in human inferior parietal lobule: Evidence from fMRI. *Neuron*, *40*, 631–642.

Committeri, G., Galati, G., Paradis, A. L., Pizzamiglio, L., Berthoz, A., & LeBihan, D. (2004). Reference frames for spatial cognition: Different brain areas

are involved in viewer-, object-, and landmark-centered judgments about object location. *Journal of Cognitive Neuroscience*, *16*, 1517–1535.

Connolly, J. D., Andersen, R. A., & Goodale, M. A. (2003). fMRI evidence for a "parietal reach region" in the human brain. *Experimental Brain Research*, *153*, 140–145.

Constantinidis, C., & Steinmetz, M. A. (2001). Neuronal responses in area 7a to multiple stimulus displays. II. Responses are suppressed at the cued location. *Cerebral Cortex*, *11*, 592–597.

Corbetta, M., Akbudak, E., Conturo, T. E., Snyder, A. Z., Ollinger, J. M., Drury, H. A., et al. (1998). A common network of functional areas for attention and eye movements. *Neuron*, *21*, 761–773.

Corbetta, M., Kincade, J. M., Ollinger, J. M., McAvoy, M. P., & Shulman, G. L. (2000). Voluntary orienting is dissociated from target detection in human posterior parietal cortex. *Nature Neuroscience*, *3*, 292–297.

Corbetta, M., Kincade, J. M., & Shulman, G. L. (2002). Neural systems for visual orienting and their relationships to spatial working memory. *Journal of Cognitive Neuroscience*, *14*, 508–523.

Cornette, L., Dupont, P., Salmon, E., & Orban, G. A. (2001). The neural substrate of orientation working memory. *Journal of Cognitive Neuroscience*, *13*, 813–828.

Culham, J. (2004). Human brain imaging reveals a parietal area specialized for grasping. In N. Kanwisher & J. Duncan (Eds.), *Functional neuroimaging of visual cognition: Attention and performance XX* (pp. 417–438). Oxford: Oxford University Press.

Culham, J. C., Brandt, S. A., Cavanagh, P., Kanwisher, N. G., Dale, A. M., & Tootell, R. B. H. (1998). Cortical fMRI activation produced by attentive tracking of moving targets. *Journal of Neurophysiology*, *80*, 2657–2670.

Culham, J. C., Cavanagh, P., & Kanwisher, N. G. (2001). Attention response functions: Characterizing brain areas using fMRI activation during parametric variations of attentional load. *Neuron*, *32*, 737–745.

Culham, J. C., Danckert, S. L., DeSouza, J. F., Gati, J. S., Menon, R. S., & Goodale, M. A. (2003). Visually guided grasping produces fMRI activation in dorsal but not ventral stream brain areas. *Experimental Brain Research*, *153*, 180–189.

Culham, J. C., & Kanwisher, N. G. (2001). Neuroimaging of cognitive functions in human parietal cortex. *Current Opinion in Neurobiology*, *11*, 157–163.

Dechent, P., & Frahm, J. (2003). Characterization of the human visual V6 complex by functional magnetic resonance imaging. *European Journal of Neuroscience*, *17*, 2201–2211.

Denys, K., Vanduffel, W., Fize, D., Nelissen, K., Peuskens, H., Van Essen, D., et al. (2004). The processing of visual shape in the cerebral cortex of human and nonhuman primates: A functional magnetic resonance imaging study. *Journal of Neuroscience*, *24*, 2551–2565.

Denys, K., Vanduffel, W., Fize, D., Nelissen, K., Sawamura, H., Georgieva, S., et al. (2004). Visual activation in prefrontal cortex is stronger in monkeys than in humans. *Journal of Cognitive Neuroscience*, *16*, 1505–1516.

Dodd, J. V., Krug, K., Cumming, B. G., & Parker, A. J. (2001). Perceptually bistable three-dimensional figures evoke high choice probabilities in cortical area MT. *Journal of Neuroscience*, *21*, 4809–4821.

Dukelow, S. P., DeSouza, J. F., Culham, J. C., van den Bergh, A. V., Menon, R. S., & Vilis, T. (2001). Distinguishing subregions of the human MT+ complex using visual fields and pursuit eye movements. *Journal of Neurophysiology*, *86*, 1991–2000.

Dupont, P., Orban, G. A., De Bruyn, B., Verbruggen, A., & Mortelmans, L. (1994). Many areas in the human brain respond to visual motion. *Journal of Neurophysiology*, *72*, 1420–1424.

Faillenot, I., Toni, I., Decety, J., Gregoire, M. C., & Jeannerod, M. (1997). Visual pathways for object-oriented action and object recognition: Functional anatomy with PET. *Cerebral Cortex*, *7*, 77–85.

Fattori, P., Gamberini, M., Kutz, D. F., & Galletti, C. (2001). 'Arm-reaching' neurons in the parietal area V6A of the macaque monkey. *European Journal of Neuroscience*, *13*, 2309–2313.

Ferraina, S., Pare, M., & Wurtz, R. H. (2002). Comparison of cortico-cortical and cortico-collicular signals for the generation of saccadic eye movements. *Journal of Neurophysiology*, *87*, 845–858.

Fize, D., Vanduffel, W., Nelissen, K., Denys, K., Chef d'Hotel, C., Faugeras, O., et al. (2003). The retinotopic organization of primate dorsal V4 and surrounding areas: A functional magnetic resonance imaging study in awake monkeys. *Journal of Neuroscience*, *23*, 7395–7406.

Fogassi, L., Ferrari, P. F., Gesierich, B., Rozzi, S., Chersi, F., & Rizzolatti, G. (2005). Parietal lobe: From action organization to intention understanding. *Science*, *308*, 662–667.

Forsssberg, H. (1999). Neural control of human motor development. *Current Opinion in Neurobiology*, *9*, 676–682.

Frey, S. H., Vinton, D., Norlund, R., & Grafton, S. T. (2005). Cortical topography of human anterior intraparietal cortex active during visually guided grasping. *Cognitive Brain Research*, *23*, 397–405.

Glimcher, P. W. (2003). The neurobiology of visual-saccadic decision making. *Annual Review of Neuroscience*, *26*, 133–179.

Gold, J. I., & Shadlen, M. N. (2003). The influence of behavioral context on the representation of a perceptual decision in developing oculomotor commands. *Journal of Neuroscience*, *23*, 632–651.

Goodale, M. A., & Milner, A. D. (1992). Separate visual pathways for perception and action. *Trends in Neuroscience*, *15*, 20–25.

Gottlieb, J. (2002). Parietal mechanisms of target representation. *Current Opinion in Neurobiology*, *12*, 134–140.

Grafton, S. T., Fagg, A. H., Woods, R. P., & Arbib, M. A. (1996). Functional anatomy of pointing and grasping in humans. *Cerebral Cortex*, *6*, 226–237.

Grefkes, C., & Fink, G. R. (2005). The functional organization of the intraparietal sulcus in humans and monkeys. *Journal of Anatomy*, *207*, 3–17.

Grefkes, C., Weiss, P. H., Zilles, K., & Fink, G. R. (2002). Crossmodal processing of object features in human anterior intraparietal cortex: An fMRI study implies equivalencies between humans and monkeys. *Neuron*, *35*, 173–184.

Huk, A. C., Dougherty, R. F., & Heeger, D. J. (2002). Retinotopy and functional subdivision of human areas MT and MST. *Journal of Neuroscience*, *22*, 7195–7205.

Indovina, I., Maffei, V., Bosco, G., Zago, M., Macaluso, E., & Lacquaniti, F. (2005). Representation of visual gravitational motion in the human vestibular cortex. *Science*, *308*(5720), 416–419.

Iriki, A., Tanaka, M., & Iwamura, Y. (1996). Coding of modified body schema during tool use by macaque postcentral neurones. *Neuroreport*, *7*, 2325–2330.

Janssen, P., & Shadlen, M. N. (2005). A representation of the hazard rate of elapsed time in macaque area LIP. *Nature Neuroscience*, *8*, 234–241.

Johansson, R. S., Westling, G., Bäckström, A., & Flanagan, J. R. (2001). Eye-hand coordination in object manipulation. *Journal of Neuroscience*, *21*, 6917–6932.

Kaas, J. (2002). Convergences in the modular and areal organization of the forebrain of mammals: Implications for the reconstruction of forebrain evolution. *Brain, Behavior and Evolution*, *59*, 262–272.

Kourtzi, Z., & Kanwisher, N. (2000). Cortical regions involved in perceiving object shape. *Journal of Neuroscience*, *20*, 3310–3318.

Koyama, M., Hasegawa, I., Osada, T., Adachi, Y., Nakahara, K., & Miyashita, Y. (2004). Functional magnetic resonance imaging of macaque monkeys performing visually guided saccade tasks: Comparison of cortical eye fields with humans. *Neuron*, *41*, 795–807.

Krubitzer, L., & Kahn, D. M. (2003). Nature versus nurture revisited: An old idea with a new twist. *Progress in Neurobiology*, *70*, 33–52.

Lacquaniti, F., Perani, D., Guigon, E., Bettinardi, V., Carrozzo, M., Grassi, F., et al. (1997). Visuomotor transformations for reaching to memorized targets: A PET study. *NeuroImage*, *5*, 129–146.

Leite, F. P., Tsao, D., Vanduffel, W., Fize, D., Sasaki, Y., Wald, L. L., et al. (2002). Repeated fMRI using iron oxide contrast agent in awake, behaving macaques at 3 Tesla. *Neuroimage*, *16*, 283–294.

Lewis, J. W., & Van Essen, D. C. (2000). Corticocortical connections of visual, sensorimotor, and multimodal processing areas in the parietal lobe of the macaque monkey. *Journal of Comparative Neurology*, *428*, 112–137.

Logothetis, N. K., Pauls, J., Augath, M., Trinath, T., & Oeltermann, A. (2001). Neurophysiological investigation of the basis of the fMRI signal. *Nature*, *412*, 150–157.

Macaluso, E., Eimer, M., Frith, C. D., & Driver, J. (2003). Preparatory states in crossmodal spatial attention: Spatial specificity and possible control mechanisms. *Experimental Brain Research*, *149*, 62–74.

Mazzoni, P., Bracewell, R. M., Barash, S., & Andersen, R. A. (1996). Motor intention activity in the macaque's lateral intraparietal area. I. Dissociation of motor plan from sensory memory. *Journal of Neurophysiology*, *76*, 1439–1456.

Murata, A., Gallese, V., Luppino, G., Kaseda, M., & Sakata, H. (2000). Selectivity for the shape, size, and orientation of objects for grasping in neurons of monkey parietal area AIP. *Journal of Neurophysiology*, *83*, 2580–2601.

Muri, R. M., Iba-Zizen, M. T., Derosier, C., Cabanis, E. A., & Pierrot-Deseilligny, C. (1996). Location of the human posterior eye field with functional magnetic resonance imaging. *Journal of Neurology, Neurosurgery, and Psychiatry*, *60*, 445–448.

Nakamura, H., Kuroda, T., Wakita, M., Kusunoki, M., Kato, A., Mikami, A., et al. (2001). From three-dimensional space vision to prehensile hand movements: The lateral intraparietal area links the area V3A and the anterior intraparietal area in macaques. *Journal of Neuroscience*, *21*, 8174–8187.

Nelissen, K., Luppino, G., Vanduffel, W., Rizzolatti, G., & Orban, G. A. (2005). Observing others: Multiple action representation in the frontal lobe. *Science*, *310*, 332–336.

Orban, G. A. (2002). Functional MRI in the awake monkey: The missing link. *Journal of Cognitive Neuroscience*, *14*, 965–969.

Orban, G. A., Fize, D., Peuskens, H., Denys, K., Nelissen, K., Sunaert, S., et al. (2003). Similarities and differences in motion processing between the human and macaque brain: Evidence from fMRI. *Neuropsychologia*, *41*, 1757–1768.

Orban, G. A., Sunaert, S., Todd, J. T., Van Hecke, P., & Marchal, G. (1999). Human cortical regions involved in extracting depth from motion. *Neuron*, *24*, 929–940.

Orban, G. A., Van Essen, D., & Vanduffel, W. (2004). Comparative mapping of higher visual areas in monkeys and humans. *Trends in Cognitive Science*, *8*, 315–324.

Paradis, A. L., Cornilleau-Pérès, V., Droulez, J., Van de Moortele, P. F., Lobel, E., Berthoz, A., et al. (2000). Visual perception of motion and 3D structure from motion: An fMRI study. *Cerebral Cortex*, *10*, 772–783.

Perry, R. J., & Zeki, S. (2000). The neurology of saccades and covert shifts in spatial attention: An event-related fMRI study. *Brain*, *123*, 2273–2288.

Petit, L., & Haxby, J. V. (1999). Functional anatomy of pursuit eye movements in humans as revealed by fMRI. *Journal of Neurophysiology*, *82*, 463–471.

Petit, L., Orssaud, C., Tzourio, N., Salamon, G., Mazoyer, B., & Berthoz, A. (1993). PET study of voluntary saccadic eye movements in humans: Basal ganglia-thalamocortical system and cingulate cortex involvement? *Journal of Neurophysiology*, *69*, 1009–1017.

Peuskens, H., Claeys, K. G., Todd, J. T., Norman, J. F., Van Hecke, P., & Orban, G. A. (2004). Attention to 3D shape, 3D motion, and texture in 3D structure from motion displays. *Journal of Cognitive Neuroscience*, *16*, 665–682.

Peuskens, H., Vanrie, J., Verfaillie, K., & Orban, G. A. (2005). Specificity of regions processing biological motion. *European Journal of Neuroscience*, *21*, 2864–2875.

Pierrot-Deseilligny, C., Rivaud, S., Gaymard, B., & Agid, Y. (1991). Cortical control of reflexive visually-guided saccades. *Brain*, *114*, 1473–1485.

Pitzalis, S., Sereno, M. I., Patria, F., Committeri, G., Galati, G., Fattori, P., et al. (2004). A possible human homologue of the macaque V6. *FENS Abstracts*, *2*, A052.18.

Platt, M. L., & Glimcher, P. W. (1999). Neural correlates of decision variables in parietal cortex. *Nature*, *400*, 233–238.

Powell, K. D., & Goldberg, M. E. (2000). Response of neurons in the lateral intraparietal area to a distractor flashed during the delay period of a memory-guided saccade. *Journal of Neurophysiology*, *84*, 301–310.

Puttemans, V., Wenderoth, N., & Swinnen, S. P. (2005). Changes in brain activation during the acquisition of a multifrequency bimanual coordination task: From the cognitive stage to advanced levels of automaticity. *Journal of Neuroscience*, *25*, 4270–4278.

Rizzolatti, G., Fadiga, L., Matelli, M., Bettinardi, V., Paulesu, E., Perani, D., et al. (1996). Localization of grasp representations in humans by PET. 1. Observation versus execution. *Experimental Brain Research*, *111*, 246–252.

Rizzolatti, G., & Luppino, G. (2001). The cortical motor system. *Neuron*, *31*, 889–901.

Rizzolatti, G., & Matelli, M. (2003). Two different streams form the dorsal visual system: Anatomy and functions. *Experimental Brain Research*, *153*, 146–157.

Rizzolatti, G., Riggio, L., Dascola, I., & Umilta, C. (1987). Reorienting attention across the horizontal and vertical meridians: Evidence in favor of a premotor theory of attention. *Neuropsychologia*, *25*, 31–40.

Sakata, H., Taira, M., Murata, A., & Mine, S. (1995). Neural mechanisms of visual guidance of hand action in the parietal cortex of the monkey. *Cerebral Cortex*, *5*, 429–438.

Sawamura, H., Georgieva, S., Vogels, R., Vanduffel, W., & Orban, G. A. (2005). Using functional magnetic resonance imaging to assess adaptation and size invariance of shape processing by humans and monkeys. *Journal of Neuroscience*, *25*, 4294–4306.

Sereno, A. B., & Maunsell, J. H. (1998). Shape selectivity in primate lateral intraparietal cortex. *Nature*, *395*, 500–503.

Sereno, M. I., Dale, A. M., Reppas, J. B., Kwong, K. K., Belliveau, J. W., Brady, T. J., et al. (1995). Borders of multiple visual areas in humans revealed by functional magnetic resonance imaging. *Science*, *268*, 889–893.

Sereno, M. I., Pitzalis, S., & Martinez, A. (2001). Mapping of contralateral space in retinotopic coordinates by a parietal cortical area in humans. *Science*, *294*, 1350–1354.

Sereno, M. I., & Tootell, R. B. H. (2005). From monkeys to humans: What do we now know about brain homologies? *Current Opinion in Neurobiology*, *15*, 135–144.

Shadlen, M. N., & Newsome, W. T. (2001). Neural basis of a perceptual decision in the parietal cortex (area LIP) of the rhesus monkey. *Journal of Neurophysiology*, *86*, 1916–1936.

Shannon, B. J., & Buckner, R. L. (2004). Functional-anatomic correlates of memory retrieval that suggest nontraditional processing roles for multiple distinct regions within posterior parietal cortex. *Journal of Neuroscience*, *24*, 10084–10092.

Shikata, E., Hamzei, F., Glauche, V., Knab, R., Dettmers, C., Weiller, C., et al. (2001). Surface orientation discrimination activates caudal and anterior intraparietal sulcus in humans: An event-related fMRI study. *Journal of Neurophysiology*, *85*, 1309–1314.

Shulman, G. L., Ollinger, J. M., Akbudak, E., Conturo, T. E., Snyder, A. Z., Petersen, S. E., et al. (1999). Areas involved in encoding and applying directional expectations to moving objects. *Journal of Neuroscience*, *19*, 9480–9496.

Silver, M. A., Ress, D., & Heeger, D. J. (2005). Topographic maps of visual spatial attention in human parietal cortex. *Journal of Neurophysiology*, *94*, 1358–1371.

Simon, O., Mangin, J.-F., Cohen, L., Le Bihan, D., & Dehaene, S. (2002). Topographical layout of hand, eye, calculation, and language-related areas in the human parietal lobe. *Neuron*, *33*, 475–487.

Smith, E. E., & Jonides, J. (1999). Storage and executive processes in the frontal lobes. *Science*, *283*, 1657–1661.

Sugrue, L. P., Corrado, G. S., & Newsome, W. T. (2005). Matching behavior and the representation of value in the parietal cortex. *Science*, *304*, 1782–1787.

Sunaert, S., Van Hecke, P., Marchal, G., & Orban, G. A. (1999). Motion-responsive regions of the human brain. *Experimental Brain Research*, *127*, 355–370.

Taira, M., Tsutsui, K.-I., Jiang, M., Yara, K., & Sakata, H. (2000). Parietal neurons represent surface orientation from the gradient of binocular disparity. *Journal of Neurophysiology*, *83*, 3140–3146.

Tehovnik, E. J., Sommer, M. A., Chou, I. H., Slocum, W. M., & Schiller, P. H. (2000). Eye fields in the frontal lobes of primates. *Brain Research Brain Research Review*, *32*, 413–448.

Terao, Y., Andersson, N. E., Flanagan, J. R., & Johansson, R. S. (2002). Engagement of gaze in capturing targets for future sequential manual action. *Journal of Neurophysiology*, *88*, 1716–1725.

Tootell, R. B., Mendola, J. D., Hadjikhani, N. K., Liu, A. K., & Dale, A. M. (1998). The representation of the ipsilateral visual field in human cerebral cortex. *Proceedings of the National Academy of Sciences of the United States of America*, *95*, 818–824.

Tootell, R. B., Reppas, J. B., Kwong, K. K., Malach, R., Born, R. T., Brady, T. J., et al. (1995). Functional analysis of human MT and related visual

cortical areas using magnetic resonance imaging. *Journal of Neuroscience*, *15*, 3215–3230.

Treue, S. (2003). Visual attention: The where, what, how and why of saliency. *Current Opinion in Neurobiology*, *13*, 428–432.

Tsao, D., & Tootell, R. (2004). Response to Tyler: Representation of stereoscopic structure in human and monkey cortex. *Trends in Neuroscience*, *27*, 118–120.

Tsao, D. Y., Vanduffel, W., Sasaki, Y., Fize, D., Knutsen, T. A., Mandeville, J. B., et al. (2003). Stereopsis activates V3A and caudal intraparietal areas in macaques and humans. *Neuron*, *39*, 555–568.

Tsutsui, K.-I., Sakata, H., Naganuma, T., & Taira, M. (2002). Neural correlates for perception of 3D surface orientation from texture gradient. *Science*, *298*, 409–412.

Vandenberghe, R., Geeraerts, S., Molenberghs, P., Lafosse, C., Vandenbulcke, M., & Peeters, K., et al. (in press). Attentional responses to unattended stimuli in human parietal cortex. *Brain*.

Vandenberghe, R., Gitelman, D. R., Parrish, T. B., & Mesulam, M. M. (2001). Functional specificity of superior parietal mediation of spatial shifting. *NeuroImage*, *14*, 661–673.

Vanduffel, W., Fize, D., Mandeville, J. B., Nelissen, K., Van Hecke, P., Rosen, B. R., et al. (2001). Visual motion processing investigated using contrast agent-enhanced fMRI in awake behaving monkeys. *Neuron*, *32*, 565–577.

Vanduffel, W., Fize, D., Peuskens, H., Denys, K., Sunaert, S., Todd, J. T., et al. (2002). Extracting 3D from motion: Differences in human and monkey intraparietal cortex. *Science*, *298*, 413–415.

Van Essen, D. (2004). Organization of visual areas in macaque and human cerebral cortex. In L. M. Chalupa & J. S. Werner (Eds.), *The visual neurosciences: Vol. 1* (pp. 507–521). MIT Press.

Vidal, M., Amorim, M.-A., & Berthoz, A. (2004). Navigating in a virtual three-dimensional maze: How do egocentric and allocentric reference frames interact? *Cognitive Brain Research*, *19*, 244–258.

Wade, A. R., Brewer, A. A., Rieger, J. W., & Wandell, B. A. (2002). Functional measurements of human ventral occipital cortex: Retinotopy and colour. *Philosophical Transactions of the Royal Society of London Series B: Biological Sciences*, *357*, 963–973.

Wandell, B., Brewer, A. A., & Dougherty, R. F. (2005). Visual field map clusters in human cortex. *Philosophical Transactions of the Royal Society of London Series B: Biological Sciences*, *360*, 693–707.

Wardak, C., Vanduffel, W., & Orban, G. A. (2005). Is there a unique LIP? A functional imaging study of saccadic representation in the parietal cortex of the awake monkey. *Society for Neuroscience Abstracts*, 590.6.

Wojciulik, E., & Kanwisher, N. (1999). The generality of parietal involvement in visual attention. *Neuron*, *23*, 747–764.

Yantis, S., Schwarzbach, J., Serences, J. T., Carlson, R. L., Steinmetz, M. A., Pekar, J. J., et al. (2002). Transient neural activity in human parietal cortex during spatial attention shifts. *Nature Neuroscience*, *5*, 995–1002.

Yantis, S., & Serences, J. T. (2003). Cortical mechanisms of space-based and object-based attentional control. *Current Opinion in Neurobiology*, *13*, 187–193.

Zeki, S., Watson, J. D., & Frackowiak, R. S. (1993). Going beyond the information given: The relation of illusory visual motion to brain activity. *Proceedings of the Royal Society of London Series B*, *252*, 215–222.

Zeki, S., Watson, J. D., Lueck, C. J., Friston, K. J., Kennard, C., & Frackowiak, R. S. (1991). A direct demonstration of functional specialization in human visual cortex. *Journal of Neuroscience*, *11*, 641–649.